Bidirectional Ca^{2+} signaling occurs between the endoplasmic reticulum and acidic organelles

Anthony J. Morgan, Lianne C. Davis, Siegfried K.T.Y. Wagner, Alexander M. Lewis, John Parrington, Grant C. Churchill, and Antony Galione

Department of Pharmacology, University of Oxford, Oxford OX1 3QT, England, UK

The endoplasmic reticulum (ER) and acidic organelles (endo-lysosomes) act as separate Ca^{2+} stores that release Ca^{2+} in response to the second messengers IP_3 and cADPR (ER) or NAADP (acidic organelles). Typically, trigger Ca^{2+} released from acidic organelles by NAADP subsequently recruits IP_3 or ryanodine receptors on the ER, an anterograde signal important for amplification and Ca^{2+} oscillations/waves. We therefore investigated whether the ER can signal back to acidic organelles, using organelle pH as a reporter of NAADP action. We show that Ca^{2+} released from the ER can activate the NAADP pathway in two ways: first, by stimulating Ca^{2+}-dependent NAADP synthesis; second, by activating NAADP-regulated channels. Moreover, the differential effects of EGTA and BAPTA (slow and fast Ca^{2+} chelators, respectively) suggest that the acidic organelles are preferentially activated by local microdomains of high Ca^{2+} at junctions between the ER and acidic organelles. Bidirectional organelle communication may have wider implications for endo-lysosomal function as well as the generation of Ca^{2+} oscillations and waves.

Introduction

A universal signal transduction mechanism for extracellular stimuli is the release of Ca^{2+} from intracellular stores (Berridge et al., 2003) with stimulus-specific Ca^{2+} patterns fine-tuned by appropriate combinations of three Ca^{2+}-mobilizing intracellular messengers: D-*myo*-inositol 1,4,5-trisphosphate (IP_3), cyclic ADP-ribose (cADPR), and nicotinic acid adenine dinucleotide phosphate (NAADP; Cancela et al., 2002; Morgan and Galione, 2008). Thus, multiple messengers entrain Ca^{2+} oscillations and waves, e.g., at fertilization (Churchill and Galione, 2001; Santella et al., 2004; Moccia et al., 2006; Whitaker, 2006; Davis et al., 2008), the activation of T cells (Steen et al., 2007; Davis et al., 2012) or pancreatic acinar cells (Cancela et al., 2002; Yamasaki et al., 2004).

While IP_3 and cADPR target their cognate receptors on the neutral sarcoplasmic or endoplasmic reticulum (SR/ER), NAADP evokes Ca^{2+} release from acidic Ca^{2+} stores (Churchill et al., 2002; Morgan et al., 2011), probably by activating complexes of the two-pore channel (TPC) family (E. Brailoiu et al., 2009, 2010a; Calcraft et al., 2009; Zong et al., 2009; Ruas et al., 2010; Morgan et al., 2011; Davis et al., 2012).

To date, the cross talk ("channel chatter"; Patel et al., 2001) between the NAADP and IP_3/cADPR pathways has centered upon "anterograde" signaling from the acidic stores to the ER in the "trigger" hypothesis (or two-pool model; Churchill and Galione, 2001): NAADP activates TPCs on acidic stores to provide the critical "pacemaker" trigger Ca^{2+} that is subsequently amplified by IP_3 receptors (IP_3Rs) and/or ryanodine receptors (RyRs) on the neutral ER/SR (Morgan et al., 2011), either via Ca^{2+}-induced Ca^{2+} release (CICR; Patel et al., 2001; Kinnear et al., 2004; Zong et al., 2009; Brailoiu et al., 2010b; Ruas et al., 2010; Davis et al., 2012) or by luminal priming (Churchill and Galione, 2001; Macgregor et al., 2007).

It is unknown whether Ca^{2+} signals travel in the reverse direction from ER to the acidic Ca^{2+} stores to make channel chatter a two-way conversation that might be important for regenerative cycles of Ca^{2+} oscillations and waves. Consequently, we have investigated whether ER (IP_3/cADPR) signals communicate with acidic Ca^{2+} stores (NAADP) by using a novel

Correspondence to Anthony J. Morgan: anthony.morgan@pharm.ox.ac.uk; or Antony Galione: antony.galione@pharm.ox.ac.uk

Abbreviations used in this paper: cADPR, cyclic ADP-ribose; CPA, cyclopiazonic acid; IP_3, inositol 1,4,5-trisphosphate; NAADP, nicotinic acid adenine dinucleotide phosphate; pH_L, luminal pH; RyR, ryanodine receptor; SERCA, sarcoendoplasmic reticulum Ca^{2+} ATPase; TPC, two-pore channel.

© 2013 Morgan et al. This article is distributed under the terms of an Attribution–Noncommercial–Share Alike–No Mirror Sites license for the first six months after the publication date (see http://www.rupress.org/terms). After six months it is available under a Creative Commons License (Attribution–Noncommercial–Share Alike 3.0 Unported license, as described at http://creativecommons.org/licenses/by-nc-sa/3.0/).

The Rockefeller University Press $30.00
J. Cell Biol. Vol. 200 No. 6 789–805
www.jcb.org/cgi/doi/10.1083/jcb.201204078

single-cell approach for monitoring acidic store activation. The activation of acidic Ca^{2+} stores is difficult to extract from cytosolic Ca^{2+} recordings that are the net result of multiple processes. This issue can be offset by monitoring the organelle lumen itself using optical reporters, e.g., targeted to ER, mitochondria, and secretory granules (Arnaudeau et al., 2001; Pinton et al., 2007; Santodomingo et al., 2008). By analogy, we have monitored the luminal pH (pH_L) of acidic Ca^{2+} stores as a readout of activation because a prompt alkalinization accompanies NAADP-induced Ca^{2+} release in sea urchin eggs (Morgan and Galione, 2007a,b; Morgan, 2011), pancreatic acinar cells (Cosker et al., 2010), and atrial myocytes (Collins et al., 2011).

Hence, we have investigated sea urchin eggs where the sperm stimulus couples to NAADP, cADPR, and IP_3 (Morgan, 2011). Given that, of these three, NAADP is unique in changing acidic store pH_L in egg homogenate and that these stores are well distributed throughout the sea urchin egg (Lee and Epel, 1983; Churchill et al., 2002; Morgan and Galione, 2007a,b; Ramos et al., 2010), we have imaged Ca^{2+} store alkalinization to "map" where and when acidic stores are activated during a physiological stimulus. Our results suggest that the ER and acidic vesicles are in close apposition and that Ca^{2+} released from the ER by IP_3/cADPR stimulates the NAADP pathway in an unexpected retrograde manner, thereby amplifying acidic Ca^{2+} store signaling. This may have profound implications for Ca^{2+} oscillations and waves in all systems.

Results

Ca^{2+} release evoked by NAADP or fertilization is accompanied by a rapid increase in the pH_L of acidic Ca^{2+} stores (Morgan and Galione, 2007a,b). In the intact sea urchin egg, this predominantly cortical pH_L response was termed a pH_LASH (pronounced "flash") that was independent of cytosolic pH changes and exocytosis (Morgan and Galione, 2007a). Because NAADP is unique in evoking this pH_L change (Morgan and Galione, 2007b), we exploited this as a "reporter" of acidic store activation (i.e., NAADP-induced Ca^{2+} release), first testing its sensitivity and spatiotemporal fidelity.

Characterizing responses to photolysis of caged NAADP

We photo-released NAADP from its microinjected caged precursor using a UV laser. No pH_L (or Ca^{2+}) responses to UV light were observed in the absence of caged NAADP (Δratio: 0.03 ± 0.01; $n = 10$, $P > 0.05$). While measuring pH_L, the uniform uncaging of NAADP (Fig. 1 A) replicated the injection of free NAADP (Morgan and Galione, 2007a), i.e., a prompt increase in the pH_L of acidic vesicles with the largest response in the cell periphery and a small but detectable response in the egg center. In contrast, when measuring Ca^{2+}, the uniform uncaging of NAADP evoked a uniform Ca^{2+} response (Fig. 1 B). However, rapid Ca^{2+} diffusion and the contribution of ER Ca^{2+} stores (Churchill and Galione, 2000) render it unsuitable for mapping acidic store activation, so we focused on pH_L as a more reliable readout.

By varying the UV laser power, the pH_L response of both the periphery and the center increased as a function of the NAADP concentration (Fig. 1 C). Indeed, when the magnitude of the responses was normalized to the maximum response, there was no difference in the sensitivity of the two regions, only in their dynamic range (Fig. 1 D). Consequently, the ratio of the responses in the periphery and center is almost invariant with NAADP concentration (the center being ∼30% of the periphery; Fig. 1 E). Kinetically, the maximal pH_LASH response (at 70% UV) occurred with a time to peak of 6.4 ± 0.4 s and a lag of 3.2 ± 0.3 s ($n = 14$). Such response times are congruent with other second messenger reporters (Nikolaev et al., 2004).

To address spatial fidelity, we focally uncaged NAADP at one pole of the egg (Fig. 1, F–H). In the majority of eggs ($n = 22$), the pH_L response precisely overlapped with the site of exposure to UV and remained at the site until it waned (Fig. 1, F–H; Fig. S1). This indicated that neither the diffusion of NAADP nor of the target vesicles themselves were confounding factors over this period. Thus, pH_L faithfully mapped experimental increases in cytosolic NAADP and acidic store activation. However, in a minority of eggs ($n = 6$) the initial, polarized response did eventually propagate to the antipode after remaining stationary at the UV site for 19 ± 3 s (Fig. S1 F). This regenerative phase clearly required positive feedback and probably reflects the secondary Ca^{2+} oscillations and waves that can be entrained by uncaging NAADP (Lee et al., 1997; Churchill and Galione, 2000, 2001).

Effect of NAADP antagonists on pH_L

If pH_L is a faithful reporter of the NAADP/TPC pathway, then responses should be inhibited by NAADP antagonists. Therefore, we tested several antagonists with the fertilization-induced pH_LASH. Note that at fertilization, the pH_L of acidic vesicles changes differently in different regions of the egg: the periphery shows a prompt alkalinization (the pH_LASH) that accompanies the main Ca^{2+} wave and can be mimicked by NAADP (Morgan and Galione, 2007a), whereas the center shows a slow acidification that is driven by an unrelated mechanism dependent upon extracellular Na^+ (Lee and Epel, 1983; Morgan and Galione, 2007a).

We first tested the fluorescent NAADP receptor antagonist, Ned-19 (Fig. S2; Naylor et al., 2009; Barceló-Torns et al., 2011). Preincubation of eggs with Ned-19 resulted in a concentration-dependent increase in Ned-19 loading, as assessed by its intrinsic fluorescence (Fig. 2 C), but which did not affect the resting pH_L (% control, 80 µM, 95 ± 2; 160 µM, 105 ± 3; $P > 0.05$, $n = 47$–83). In keeping with a role for NAADP, Ned-19 inhibited the sperm-induced pH_LASH (Fig. 2, A–C). This was not due to a general interference with fertilization because it had little effect upon the slower acidification of the central acidic granules (Fig. 2, A–C; Lee and Epel, 1983; Morgan and Galione, 2007a) or upon fertilization envelope lifting driven by the other remaining fertilization messengers, cADPR and IP_3 (Fig. 2 B, inset). Furthermore, we confirmed that Ned-19 inhibited the pH_LASH evoked by injection of NAADP itself (Fig. 2 D).

Unlike RyRs and IP_3Rs, NAADP receptors are inhibited by high concentrations of L-type Ca^{2+} channel blockers in sea urchin egg and other cell types (Genazzani et al., 1997; Mándi et al., 2006; Zhang and Li, 2007). Conveniently, both the main fertilization-induced Ca^{2+} wave (Shen and Buck, 1993) and the

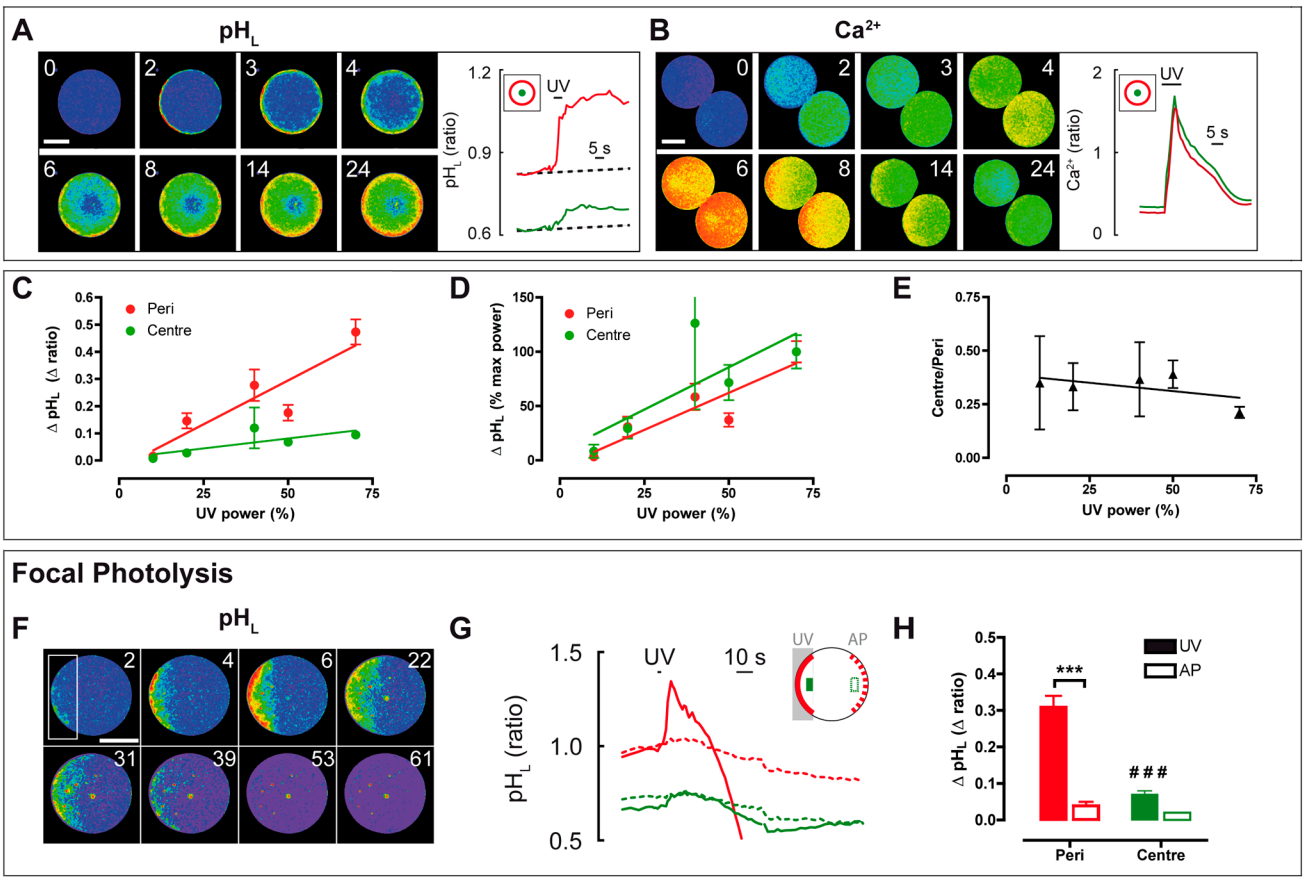

Figure 1. **Characterization of pH_L changes in response to photolysis of caged NAADP.** Sea urchin eggs were microinjected with caged NAADP (~0.5 µM cytosolic concentration) and photolysis effected with a UV laser as indicated. Images are pseudocolored ratios of one channel (pH_L) or two channels (Ca^{2+}), and time after photolysis indicated in seconds in the corner. The inset cartoons indicate the regions of interest from which the traces are derived. (A) In ratiometric pH_L recordings, global photolysis (70% UV) evoked a larger response in the periphery (red) than the center (green). $n \geq 14$ eggs. (B) Ratiometric Ca^{2+} recordings. The traces correspond to the bottom cell exposed globally to 70% UV laser. $n \geq 6$ eggs. (C) Quantification of the initial rapid pH_L responses in the periphery (red) and center (green) as a function of UV intensity. Data are mean ± SEM of 3–19 eggs. (D) Same data as C normalized to the maximal pH_L response recorded in each region. (E) Magnitude of the central response as a percentage of the corresponding peripheral change. (F) Focal uncaging of NAADP elicits a pH_L response (50% UV, irradiated at box indicated). (G) pH_L changes at the UV site (solid line) and antipode (dotted line) in the periphery and center. (H) Summary of changes at the UV site (UV) and antipode (AP); mean ± SEM of $n = 22$ eggs (***, $P < 0.001$; ###, $P < 0.001$ compared with Peri UV). Bars, 50 µm.

pH_LASH itself (Fig. S2 E) are independent of Ca^{2+} influx. As a selective NAADP antagonist (Fig. S2, A and B), the phenylalkylamine, diltiazem, selectively inhibited the sperm-induced pH_LASH compared with the central acidification (Fig. 2 F) and, like Ned-19, did not interfere with fertilization envelope lifting (unpublished data). Diltiazem also inhibited the responses to NAADP injection in terms of the pH_LASH and fertilization envelope lifting (consistent with a block of Ca^{2+} release, Fig. 2 G).

Similarly, another L-type Ca^{2+} channel blocker, nifedipine (a dihydropyridine), also inhibited the sperm-induced pH_LASH (but not the central acidification, Fig. 2 E). This partial inhibition by nifedipine was at its limit of solubility and probably reflects its lower membrane permeability compared with diltiazem (XlogP3 of 2.2 and 3.1, respectively). Finally, the nucleotide mimetic, PPADS, inhibited NAADP responses (Fig. S2; Billington and Genazzani, 2007) and selectively inhibited the pH_LASH when microinjected into the egg, precluding an extracellular site of action (Fig. 2 E). Together, the data affirm NAADP as the main pH_L messenger at fertilization and strengthen pH_L as a physiologically relevant reporter of the NAADP pathway.

Ca^{2+} drives NAADP synthesis and pH_L responses

With a means of mapping acidic store activation, we asked whether Ca^{2+} released from the ER can signal to acidic vesicles. First, we elevated Ca^{2+} independently of sperm using ionomycin, a Ca^{2+} ionophore that mobilizes Ca^{2+} from neutral (and not acidic) Ca^{2+} stores (Fasolato et al., 1991; see Fig. 5 A) and which acts only weakly at the plasma membrane (Morgan and Jacob, 1994). Ionomycin evoked a prompt Ca^{2+} rise in eggs (Fig. 3, Eii), as well as a pH_LASH (Fig. 3, Ei). However, the pH_L response was slower, mimicking the sperm response in its magnitude (Fig. 3, A–C) and kinetics (time to peak (s) ionomycin: 69 ± 2; sperm: 60 ± 2; n = 31–39). Because ionomycin has no direct effect upon the pH_L of sea urchin egg acidic vesicles (Morgan and

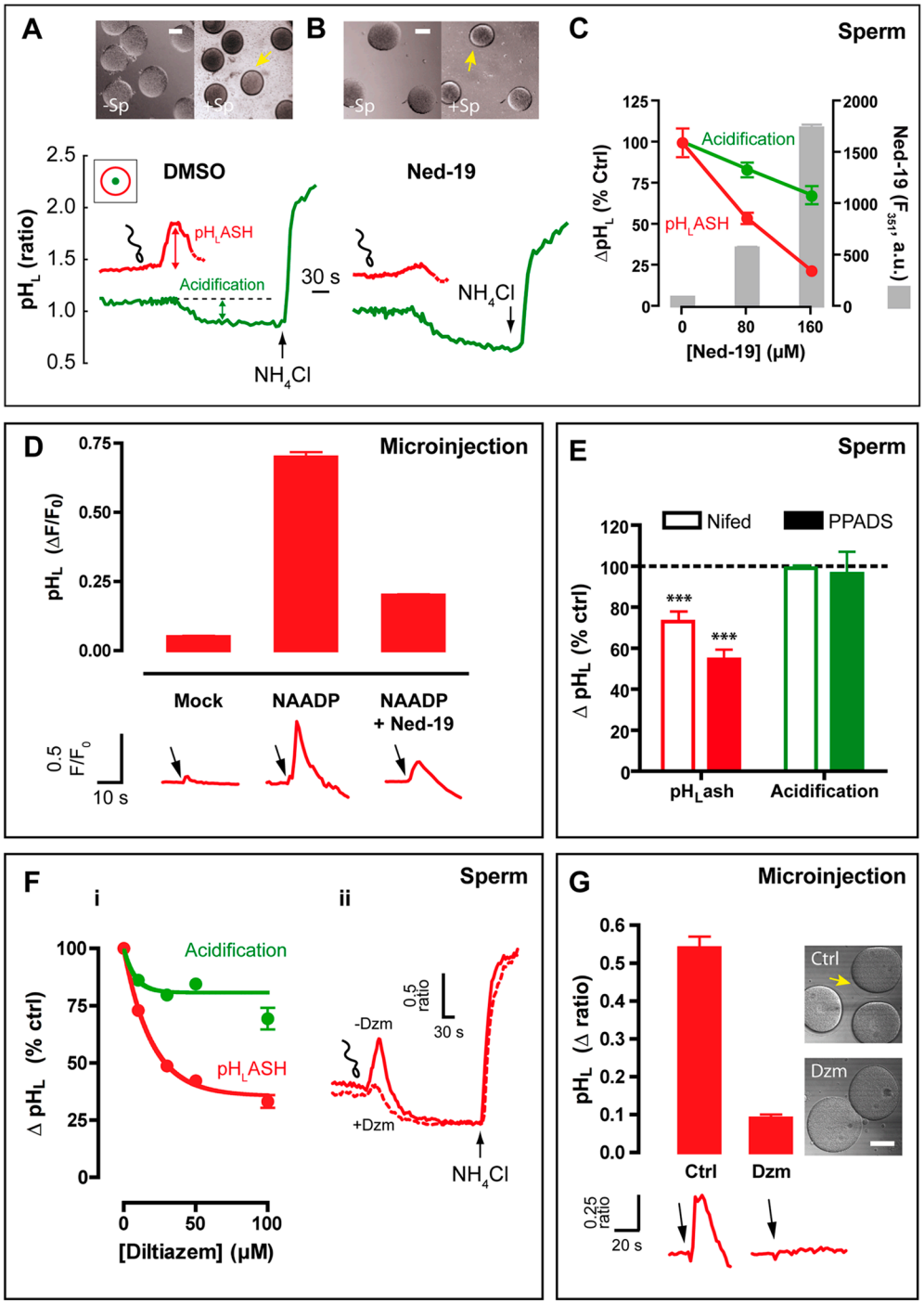

Figure 2. **Inhibition of the NAADP receptor inhibits the fertilization-induced pH$_L$ASH.** (A–C) Ned-19 was preincubated with eggs for 30 min (at 80 μM) or 60–90 min (at 160 μM) or with DMSO vehicle (0.16% vol/vol) as a control. Eggs were loaded with Acridine orange plus LysoTracker red for the final 15–20 min of the preincubation period. Peripheral (red) and central (green) pH$_L$ responses to sperm in single eggs treated with DMSO (A) or 160 μM Ned-19 (B). At the end, 10 mM NH_4Cl was applied. Inset brightfield images show unfertilized (minus sperm, −Sp) and fertilized eggs (plus sperm, +Sp), with the yellow arrows highlighting the boundary of the fertilization envelope. Bars, 50 μm. (C) Summary of the effect of Ned-19 on the rapid pH$_L$ASH (red) and central slow central acidification (green) expressed as the percentage of DMSO-treated eggs; n = 45–83 eggs. The bar chart (gray boxes) quantifies Ned-19 loading into single eggs measured as its intrinsic fluorescence at 351 nm (n = 77–130 eggs). (D) Effect of Ned-19 (160 μM, 30 min) upon the pH$_L$ response to microinjection of free NAADP (50 μM pipette). Eggs loaded with Acridine orange were injected with Alexa Fluor 647 dextran alone (Mock), or Alexa Fluor 647 dextran plus NAADP. Bar chart summarizes the pH$_L$ASH in 8–28 eggs, the underlying traces normalized to their initial fluorescence. (E) Summary of the effect of nifedipine and PPADS on pH$_L$ responses to sperm, normalized to the respective responses in untreated eggs. 100 μM nifedipine (or DMSO) was included during the dye-loading period (20 min), n = 28–102 eggs; PPADS (10 mM pipette) was microinjected into dye-loaded eggs, n = 39–45. (F) Effect of diltiazem upon sperm-induced pH$_L$ changes. (Fi) Diltiazem was included during the dye-loading period (20 min), and responses normalized to the peripheral pH$_L$ASH or central acidification responses in control eggs (Ctrl) in the absence of inhibitor (n = 64–426 eggs). (Fii) Peripheral pH$_L$ records in the absence or presence of 50 μM diltiazem (±Dzm). NH_4Cl = 10 mM. Traces are the mean of 19 (−Dzm) or 36 (+Dzm) eggs, respectively. (G) Preincubation with 50 μM diltiazem inhibited the response to NAADP injection (50 μM pipette), both in terms of the peripheral pH$_L$ASH (bar chart) and fertilization envelope lifting (inset micrographs); n = 11–12. Bar, 50 μm.

Galione, 2007b) it follows that it is the released Ca^{2+} that affects acidic vesicles.

Their relative kinetics imply that the pH_LASH is downstream of Ca^{2+} and this is consistent with the one mirroring the other in space: the pH_L (Fig. 3, Di) and Ca^{2+} (Fig. 3, Dii) responses to sperm each occurred as waves (that propagate away from the sperm entry point; Morgan and Galione, 2007a), whereas ionomycin induced a synchronous cortical elevation of either pH_L or Ca^{2+} (Fig. 3, Ei and ii). Taken together, the kinetic and spatial interrelationship of the two parameters is consistent with Ca^{2+} driving pH_L changes.

How could the Ca^{2+} released by ionomycin be stimulating acidic vesicles? As argued previously for sperm (Morgan and Galione, 2007a), the pH_LASH is not limited by the time of the acidic stores to respond to NAADP (an ~10-times faster process), so the kinetics may reflect the time taken to generate NAADP. We therefore tested whether ionomycin could elevate NAADP levels, as measured in populations of eggs with a radioreceptor assay (Lewis et al., 2007). As observed previously, fertilization increased NAADP in two phases: the first phase represents an increase in NAADP in the sperm as they contact the egg jelly, the second phase is due to de novo synthesis of NAADP inside the egg (Fig. 3 F; Churchill et al., 2003). Remarkably, ionomycin increased NAADP in eggs with kinetics that not only overlapped with the second "egg" phase but also that mirrored the slow time to peak of the pH_L response (each peaked at ~70 s; Fig. 3 F). The maximum magnitude of the ionomycin-evoked NAADP increase was variable between preparations, being 30 ± 18% ($n = 4$) of that evoked by sperm.

If ionomycin increases NAADP, then its pH_LASH should be sensitive to NAADP inhibitors. We also used SKF96365 to block NAADP (Moccia et al., 2004; Bezin et al., 2008) after first confirming its >50-fold selectivity for NAADP over cADPR and IP_3 (Fig. S2, C and D). Although SKF96365 could not be used with sperm because it blocks sperm chemotaxis and the acrosome reaction (Hirohashi and Vacquier, 2003; Yoshida et al., 2003; Treviño et al., 2006), it was an effective inhibitor of the ionomycin-induced pH_LASH (Fig. 3 I). Similarly, Ned-19 and diltiazem also inhibited the ionomycin pH_LASH (Fig. 3, G and H) with a similar potency (and selectivity over the slow central acidification) to that seen against the sperm-induced response (Fig. 2, C and F). The data suggest that Ca^{2+} release from the ER by ionomycin can stimulate a pH_LASH via NAADP generation and action.

ER channel activation evokes a pH_LASH

We next investigated if more physiological routes of Ca^{2+} release from the ER could support acidic store activation. Sea urchin eggs are sensitive to both ER-targeting messengers, IP_3 and cADPR (Churchill and Galione, 2001; Morgan and Galione, 2007b), and we first confirmed that microinjection of these messengers elicited robust Ca^{2+} responses similar to those with NAADP itself (Fig. 4, A and B). When subsequently measuring pH_L changes, not only did NAADP evoke a pH_LASH but so did cADPR and IP_3 (Fig. 4, C and D). Although the examples shown are among the best responses seen with cADPR and IP_3, overall they were weaker stimuli of the pH_LASH than was NAADP (Fig. 4 E), with IP_3 being the least efficacious. This differential messenger profile for the pH_LASH contrasted with the similar global Ca^{2+} responses (Fig. 4, A and B). The fact that IP_3 and cADPR do not directly affect pH_L in egg homogenate (Morgan and Galione, 2007b) implies that these receptors do not reside on acidic vesicles themselves, and that the mechanism that normally couples Ca^{2+} to pH_L is lost upon homogenization.

Differential coupling of Ca^{2+} signals to the pH_LASH

Such differential coupling of second messengers to the pH_LASH might be explained by local Ca^{2+} domains; i.e., a high local Ca^{2+} required for a pH_LASH might be readily attained by NAADP but less so by cADPR and IP_3. We therefore tested whether other Ca^{2+} signals differentially couple to the pH_LASH. First, release of Ca^{2+} from the ER was evoked by inhibiting SERCA (sarco-endoplasmic reticulum Ca^{2+} ATPase) with cyclopiazonic acid (CPA). In most cells, CPA stimulated a small, slow Ca^{2+} release (Fig. 5, A–C) that failed to evoke a pH_LASH (Fig. 5, D–F), even though a subsequent addition of ionomycin was successful (Fig. 5, D–F). This is consistent with the CPA-induced Ca^{2+} rise failing to reach a local Ca^{2+} threshold. Nonetheless, in ~28% of cells, CPA produced a secondary peak of Ca^{2+} release after a long delay (285 ± 24 s; Fig. 5, A–C) that translated into a pH_LASH after 361 ± 15 s. Overall, CPA coupled weakly to a pH_LASH.

In contrast to CPA, photolysis of caged Ca^{2+} elicited a very rapid increase in Ca^{2+} whose amplitude was indistinguishable ($P > 0.05$) from that produced by sperm (Fig. 5, G–I). However, in spite of the globally similar Ca^{2+} signals, the photolysis of caged Ca^{2+} failed to produce a pH_LASH in 90% of eggs (only two eggs gave a pH_LASH; Fig. 5, J–L). This weak coupling provides strong evidence that it is the local and not global Ca^{2+} that is an important determinant of the coupling efficiency.

Ca^{2+} release from the ER stimulates NAADP receptors

We then asked what mechanism couples IP_3/cADPR to a pH_LASH, with potential pathways depicted in Fig. 6 A. We first tested whether ER Ca^{2+} recruits the NAADP pathway by using three NAADP receptor antagonists. At concentrations that block NAADP itself, Ned-19, diltiazem, and SKF96365 also inhibit the pH_LASH response to both cADPR and IP_3 (Fig. 6, B and C). This places NAADP action downstream of ER Ca^{2+} because the inhibitors do not affect Ca^{2+} release evoked by IP_3 or cADPR (Fig. S2; Genazzani et al., 1997; Naylor et al., 2009), as confirmed by the weak effect of the inhibitors upon Ca^{2+}-dependent exocytosis (fertilization envelope lifting; Fig. 6 D). We therefore exclude pathway 2 (Fig. 6 A).

Because IP_3Rs and RyRs are on the ER, Ca^{2+} must diffuse from the ER to target sites that affect acidic stores, and this should be blocked by EGTA. Accordingly, EGTA ablated the pH_LASH response to either cADPR or IP_3 (Fig. 6, B and C). This contrasted with the robust pH_L response to NAADP in the presence of EGTA (Fig. 6, B and C; Morgan and Galione, 2007b). The data suggest that IP_3 and cADPR stimulate acidic stores after Ca^{2+} diffusion from the ER to target domains (Fig. 6 A, pathway 1 or 3).

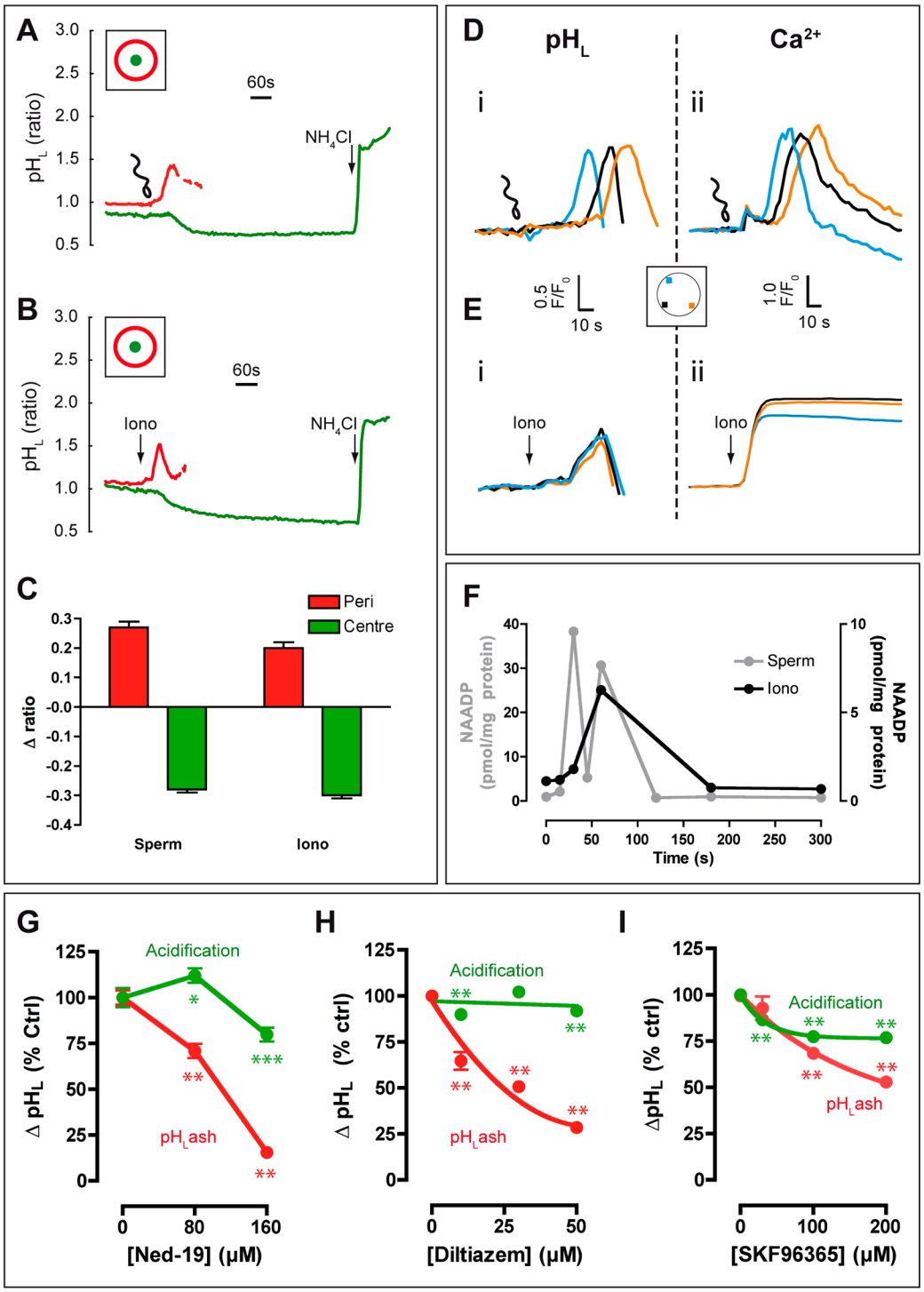

Figure 3. **Ca^{2+} increases pH_L and NAADP levels.** (A–E) Eggs loaded with Acridine orange and LysoTracker red were exposed to sperm, 1 µM ionomycin, or 10 mM NH_4Cl. Representative traces of the peripheral (red) and central (green) pH_L changes with sperm (A) or ionomycin (B). Exocytosis results in movement out of the peripheral ROI (Morgan and Galione, 2007a), hence the break in the red traces. (C) Summary of the rapid peripheral pH_{LASH} (red) and the slow central acidification (green) responses with sperm and ionomycin, *n* = 48–49 eggs. (D and E) Spatial nature of the single-cell peripheral pH_L (*n* = 48–49 eggs) and Ca^{2+} (*n* = 8–21 eggs) responses to sperm (top) and ionomycin (bottom). For clarity, traces are normalized to the initial (F_0) Acridine orange or rhod-dextran fluorescence and derived from the three regions of interest illustrated in the inset egg schematic. (F) NAADP levels measured in populations of eggs stimulated by sperm (gray) or 1–2 µM ionomycin (black). Data are from a single preparation, typical of four. (G–I) Effect of NAADP antagonists on 1–2 µM ionomycin-induced pH_L changes. Ned-19 (*n* = 40–60 eggs) and diltiazem (*n* = 91–200 eggs) were preincubated according to the protocols in Fig. 2; SKF96365 (or 0.1–0.2% DMSO vehicle) was coincubated with the pH_L dyes in the presence of 0.05% Pluronic F127 to promote inhibitor loading (*n* = 72–428 eggs). NAADP antagonists had a significantly greater effect upon the pH_{LASH} than the acidification ($P < 0.001$) at all concentrations except 30 µM SKF96365 ($P > 0.05$). *, $P < 0.05$; **, $P < 0.01$; ***, $P < 0.001$ vs. 0 µM control.

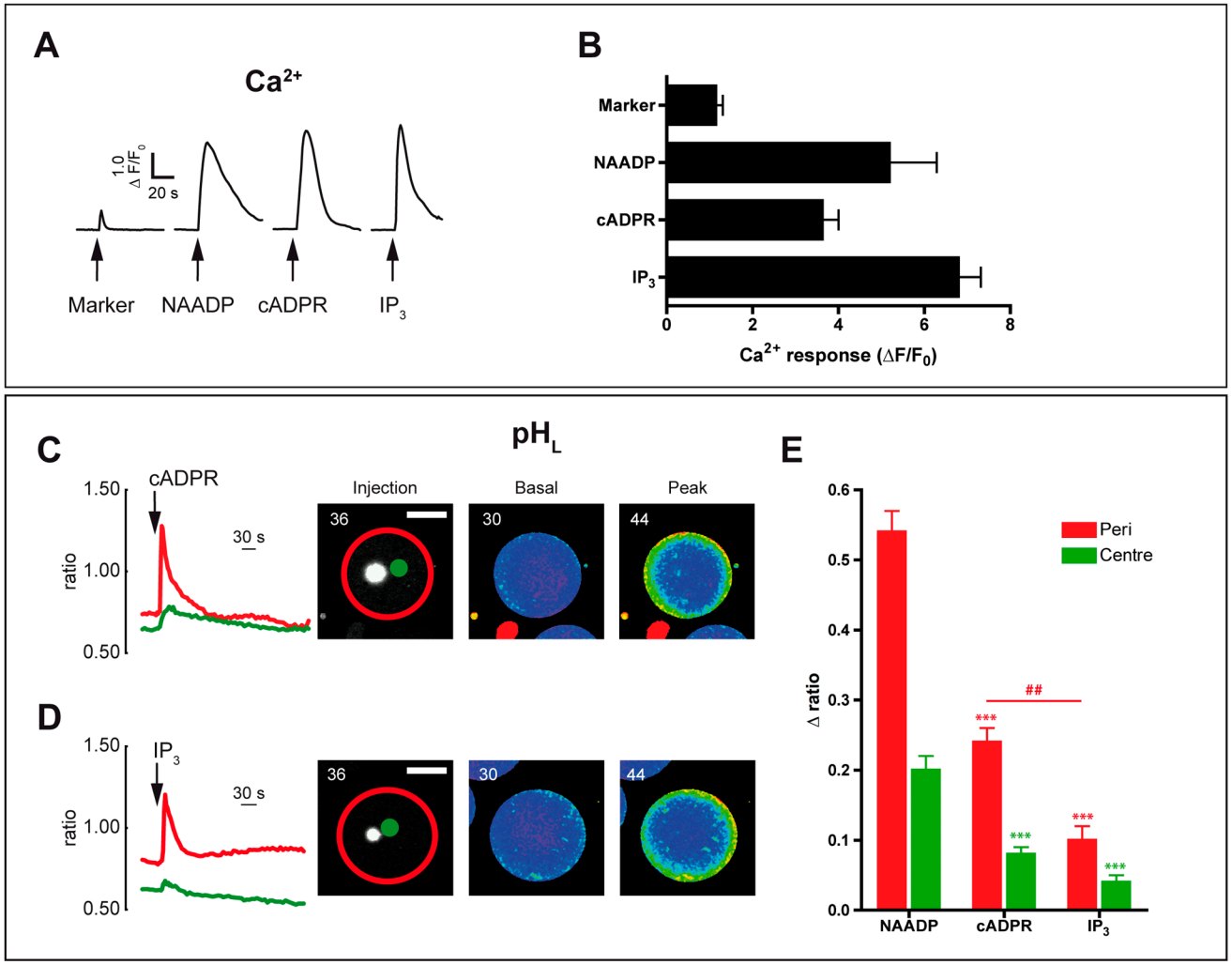

Figure 4. **ER messengers increase Ca^{2+} and pH_L.** (A) Ca^{2+} responses to messenger injection. Eggs preinjected with fluo-4-dextran were injected using a second pipette containing injection marker alone (50 µM Alexa Fluor 647 dextran, "Marker") or marker plus 50 µM NAADP, 30 µM cADPR, or 1 mM IP_3. Ca^{2+} responses were normalized to the resting fluorescence. (B) Summary of maximum amplitudes, n = 5–10 eggs. (C and D) Microinjection of cADPR or IP_3 into eggs loaded with Acridine orange and LysoTracker red. Bar, 50 µm. The fluorescence of the injection marker (Alexa Fluor 647 dextran) indicated the time and site of injection ("Injection" image). The basal and peak images are pseudocolored ratio images corresponding to the adjacent traces, which are color matched to the ROIs drawn on the injection image. (E) Maximum increases in the peripheral (red) or central (green) pH_L signal in response to the same messenger concentrations stated above. Data are mean ± SEM of 57–84 eggs. ***, $P < 0.001$ vs. corresponding NAADP response; ##, $P < 0.01$.

Interestingly, EGTA did slightly modify the response to NAADP, reducing the amplitude (Fig. 5, B and C) and slowing the upstroke kinetics (time to peak [s]: Ctrl, 6 ± 0; EGTA, 28 ± 3; $P < 0.001$). The fact that EGTA (a slow Ca^{2+} buffer) strongly inhibited the IP_3/cADPR pH_{LASH} but was weaker toward the NAADP pH_{LASH} was further evidence of local Ca^{2+} domains around acidic vesicles facilitating the pH_{LASH}. As a final confirmation, we tested the fast Ca^{2+} buffer, BAPTA, which is able to dissipate Ca^{2+} gradients in microdomains (Kidd et al., 1999; G. Brailoiu et al., 2009). The NAADP-induced pH_{LASH} was almost completely abolished by BAPTA (Fig. 6, B and C). We conclude that Ca^{2+} release by NAADP evokes locally high Ca^{2+} concentrations around the acidic vesicles that are required for acidic vesicle activation (alkalinization). Together the data support the main highlighted pathway 3 in Fig. 6 A in which IP_3- or cADPR-induced Ca^{2+} release from the ER activates acidic vesicles via the Ca^{2+}-sensitive NAADP pathway.

Heterologous desensitization

To complement NAADP inhibition, we examined the effect of NAADP receptor desensitization. Microinjection of NAADP into the egg demonstrably desensitized both the Ca^{2+} and pH_{LASH} responses to a second NAADP injection (Fig. 7, Ai and Ci); crucially, NAADP desensitization inhibited the IP_3-induced pH_{LASH} (Fig. 7, Ciii) without affecting IP_3-induced Ca^{2+} release (Fig. 7, Aiii). Thus, desensitization uncoupled IP_3-induced Ca^{2+} release from the pH_{LASH} and mimicked the action of NAADP antagonism.

Conversely, if IP_3 recruits NAADP receptors, then injection of IP_3 first should cross-desensitize them. We found that both the Ca^{2+} (Fig. 7, Aiv) and pH_{LASH} (Fig. 7, Civ) responses to NAADP were reduced by prior IP_3 injection, consistent with heterologous desensitization of the NAADP receptors.

Unfortunately, the analogous cross-desensitization of the cADPR pH_{LASH} response was not technically possible because

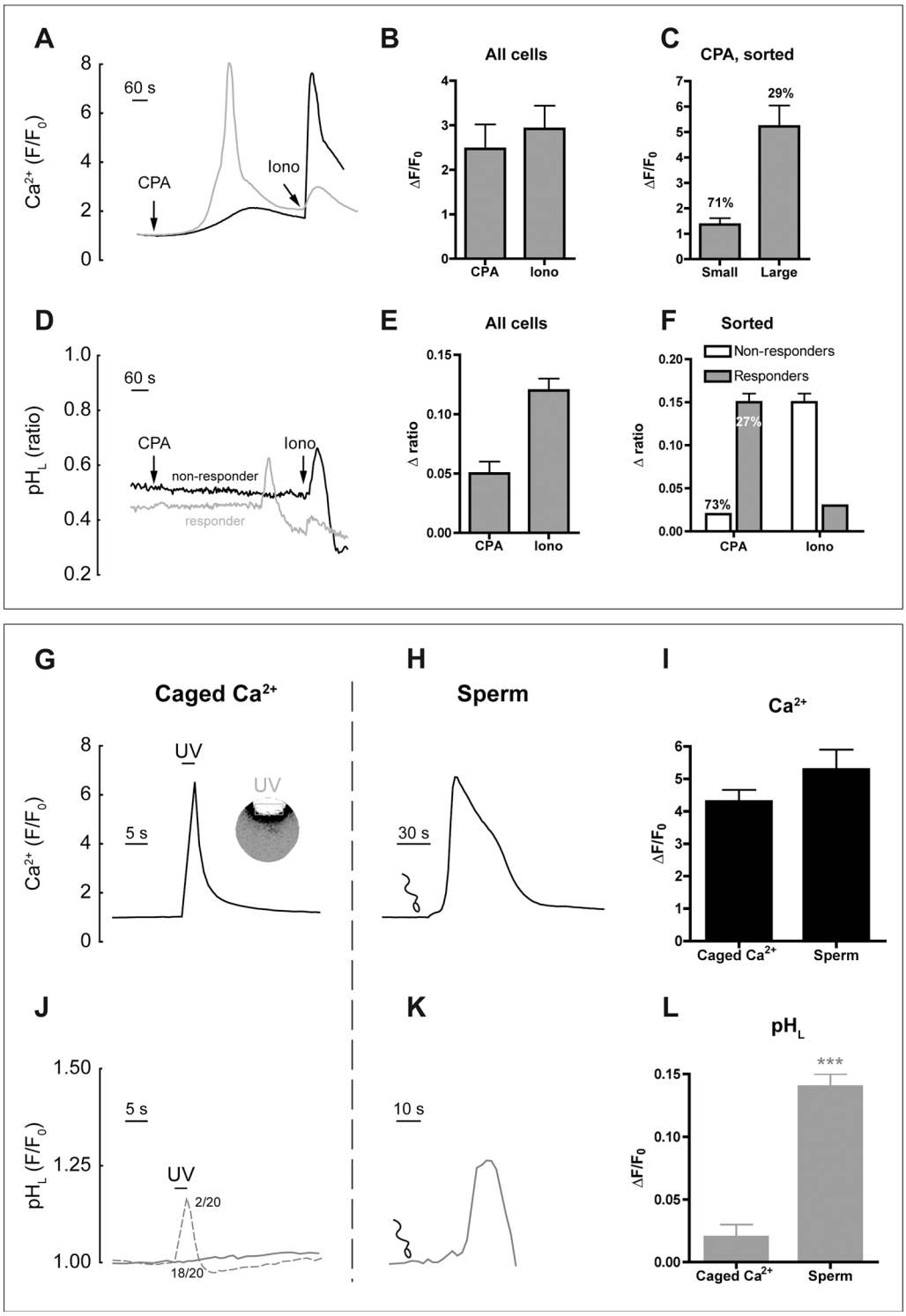

Figure 5. **SERCA inhibition and caged Ca^{2+} couple weakly to the pH_{LASH}.** (A–C) Effect of the SERCA inhibitor, cyclopiazonic acid (CPA, 150 µM) upon Ca^{2+}. (A) Two types of single-cell CPA responses were observed: a predominant small, monotonic increase (black trace) or a large, biphasic increase (gray trace). 2 µM ionomycin (iono) was then added. (B) Bar chart summarizing the peak responses from all cells (n = 14). (C) Summary of CPA responses sorted into the two categories with the percentage of eggs exhibiting them indicated above the bars. (D–F) CPA is a poor pH_{LASH} stimulus. (D) Most eggs failed to give a pH_L response to 150 µM CPA (nonresponders, black trace), but a minority showed a peripheral pH_{LASH} after a delay. (E) Summary of peak responses in all eggs (n = 132). (F) Data were categorized as CPA responders (n = 35) or CPA nonresponders (n = 97) and the CPA and subsequent ionomycin responses plotted accordingly (the percentage of eggs is indicated). (G–I) Comparison of caged Ca^{2+} and fertilization upon Ca^{2+} signals in eggs. (G) Eggs were injected with caged Ca^{2+} (NP-EGTA, ~250 µM cytosolic) and focal photolysis initiated in a cortical region of the egg by UV laser. The trace represents the Ca^{2+} response within the photolysis region; the inset shows the Ca^{2+} peak in a single egg as an F/F_0 image, with the photolysis region of interest labeled as "UV". (H) Whole-cell Ca^{2+} signal in response to sperm. (I) Summary of peak Ca^{2+} amplitudes (n = 24, caged Ca^{2+} ; n = 7, sperm). (J and K) pH_{LASH} response to photolysis of caged Ca^{2+} (J) or sperm (K). Most cells (18/20) did not respond to uncaging, only 2/20 cells gave a pH_{LASH} (J, dotted line). (L) Summary of the peak pH_L responses in all cells (n = 20, caged Ca^{2+}; n = 64, sperm). ***, $P < 0.001$ compared with uncaging.

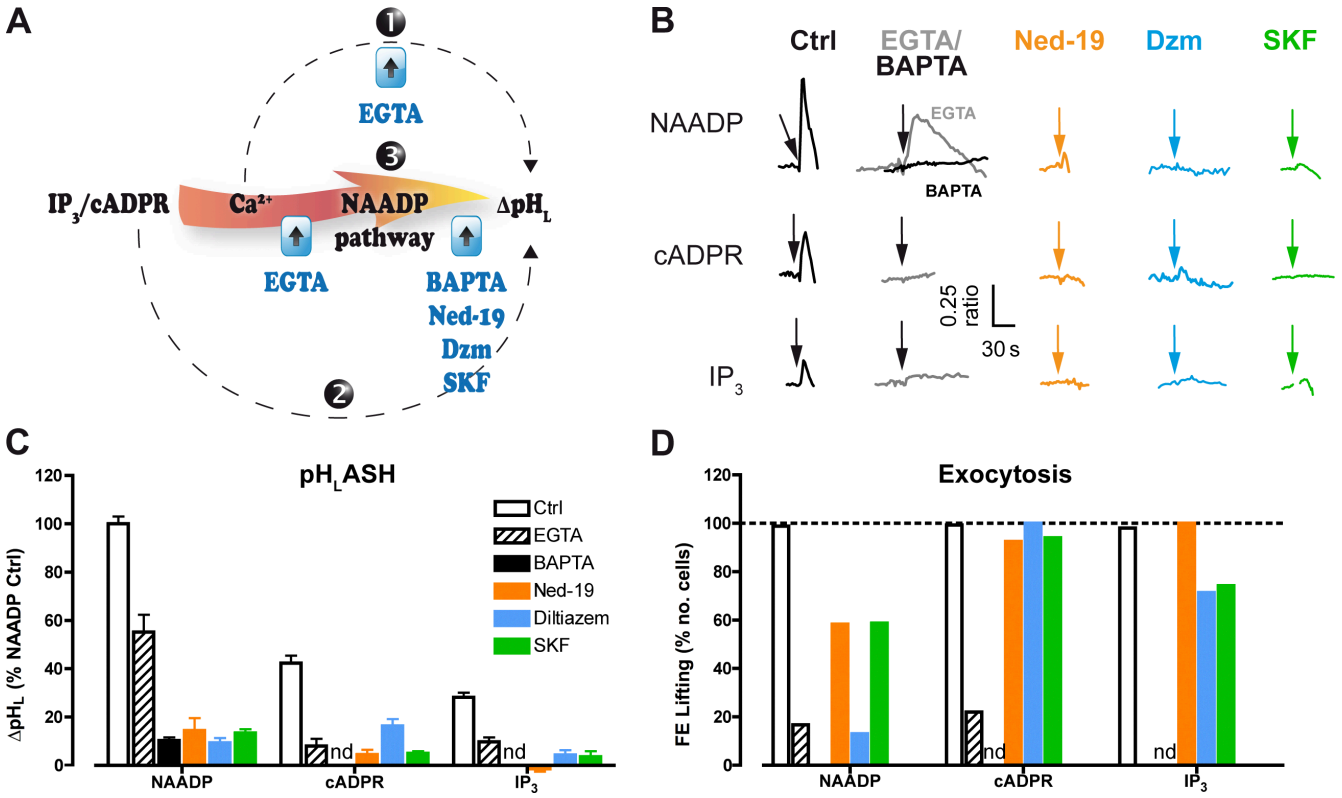

Figure 6. **Pharmacology of pH_L responses and fertilization envelope lifting.** (A) Schematic indicating the possible routes that IP_3 and cADPR could affect pH_L. (B) Representative traces of the pH_L responses to messenger injection (pipette concentrations, 50 µM NAADP, 20–30 µM cADPR, and 1 mM IP_3). Left-hand column shows control (Ctrl) responses in the absence of inhibitors (but in the presence of vehicle). Other columns depict egg treatment: injected with EGTA or BAPTA (pipette concentrations of 250 mM); preincubated for 60 min with 160 µM Ned-19; preincubated with 50 µM diltiazem (Dzm); or 200 µM SKF96365 (plus 0.05% Pluronic F127) during dye loading for 15–20 min. (C) Summary of the messenger-induced pH_LASH expressed as a percentage of the NAADP control (Ctrl); n = 9–124 eggs. (D) Quantification of fertilization envelope lifting in the same eggs as pH_L was recorded. Data are expressed as the number of eggs that showed a partial/full lifting as a percentage of the total number of eggs injected with each messenger. The effect of BAPTA on cADPR and IP_3 was not determined (nd).

when NAADP was injected first, the subsequent cADPR-induced Ca^{2+} release was profoundly cross-desensitized (Fig. S3), probably reflecting the secondary recruitment of the cADPR pathway by NAADP (Churchill and Galione, 2000) and its consequent, persistent desensitization (Thomas et al., 2002). Nonetheless, the data overall support our model of bidirectional communication.

Fertilization uses bidirectional Ca^{2+} signaling

The corollary of such cross talk is that ER Ca^{2+} is important physiologically for facilitating acidic store activation via NAADP. We first tested whether cytosolic Ca^{2+} was important for the pH_LASH by microinjecting eggs with EGTA. After verifying that EGTA blocked the Ca^{2+} response at fertilization (Fig. 8 A), we showed that it did indeed inhibit the pH_LASH (when measured throughout the entire periphery; Fig. 8 B). However, when analyzed more closely, some eggs injected with EGTA showed a highly localized, nonpropagating pH_L increase (Fig. 8, C and D). Moreover, this "hot spot" coincided with the point of sperm contact (Fig. 8 C, inset) and may correspond to the bolus of NAADP delivered to the egg by sperm (see Discussion; Churchill et al., 2003). An additional hot spot of pH_L was observed in another part of the egg periphery (presumably due to polyspermy when fertilization envelope lifting is inhibited by EGTA). This suggests that Ca^{2+} is physiologically important for propagating acidic store activation, apparently by amplifying the initial sperm-induced trigger.

We then tested whether this facilitating Ca^{2+} was released from the ER by IP_3/cADPR. Consequently, fertilization was effected in eggs that had been microinjected with a cocktail of IP_3 and cADPR antagonists (heparin and 8-NH_2-cADPR, respectively; Churchill and Galione, 2000) or with an injection marker alone. In the absence of inhibitors, the pH_LASH proceeded as a wave away from the point of sperm entry (Morgan and Galione, 2007a) to be subsequently mirrored in the antipode (Fig. 3, Di; Morgan and Galione, 2007a). One would predict that the effect of blocking ER Ca^{2+} release would be similar to microinjecting EGTA and, qualitatively, this is what we observed: a nonpropagating, local pH_L response remained at one pole of the cell (Fig. 8, E and F) that was smaller in amplitude (Fig. 8 G) and slower (Fig. 8 H) than the initiation site response in control eggs. These data are consistent with ER Ca^{2+} release amplifying acidic store activation during fertilization.

Acidic vesicle/ER junctions

These functional data imply a close physical apposition of acidic Ca^{2+} stores and the ER that was borne out by examining the cellular architecture. In the cortex where the pH_LASH was observed, acidic vesicles and ER were densely packed and,

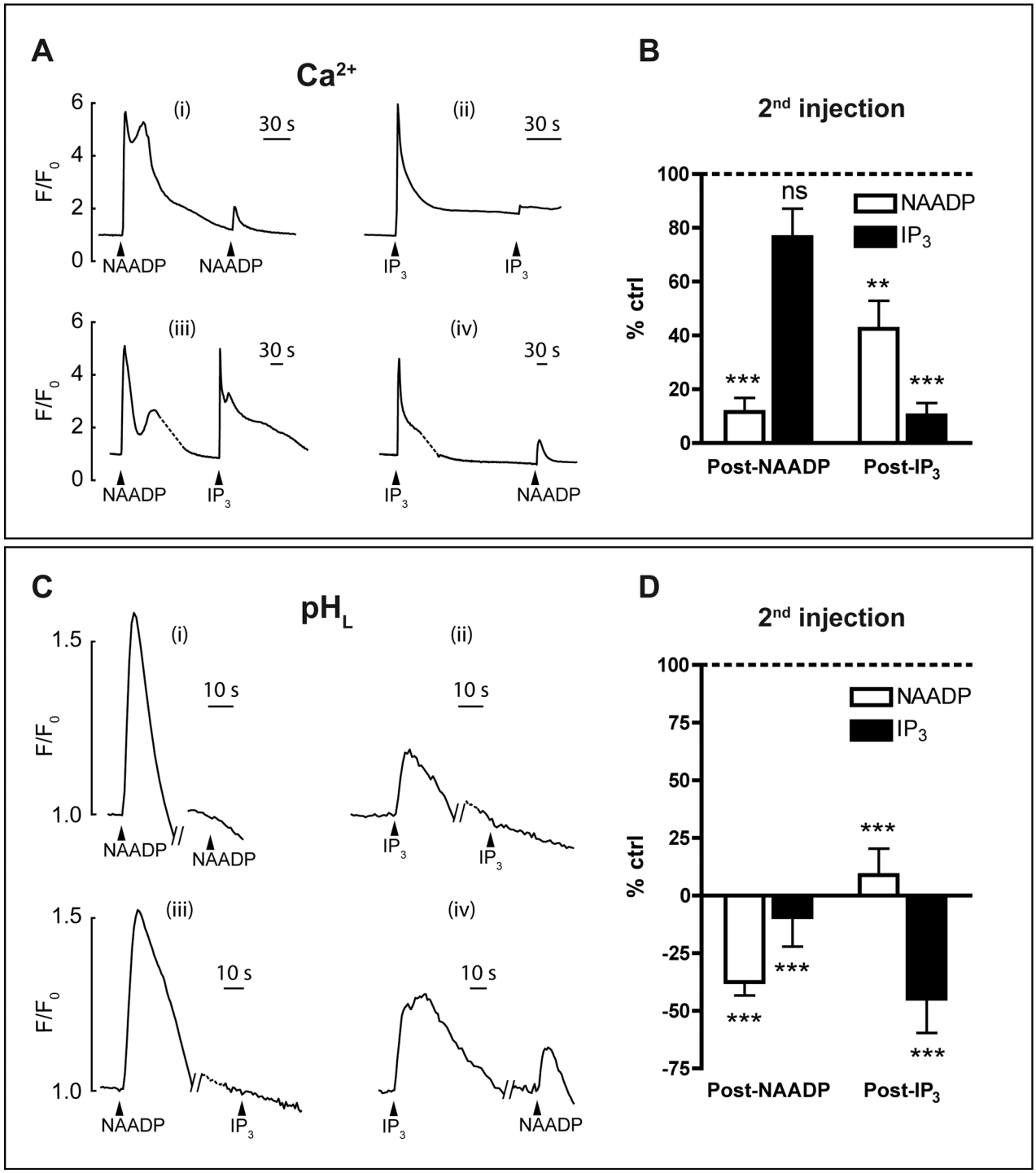

Figure 7. **Cross-desensitization of NAADP and IP_3 responses.** Second messengers were consecutively injected into intact eggs and either Ca^{2+} (A and B) or pH_{LASH} (C and D) monitored. Injectate contained either 50 µM NAADP or 1 mM IP_3. Breaks in the recordings reflect the change of micropipette and/or cell shape. Data were quantified as a percentage of the control NAADP or IP_3 responses. Bar charts (B and D) depict the response to the second injection of the pair and are the mean ± SEM. Ca^{2+} control responses of n = 18–24 eggs; second NAADP (n = 5–10), IP_3 (n = 8–19). pH_L controls of n = 124–151 eggs; second NAADP (n = 29–53), IP_3 (n = 24–61). ns, not significant; **, P < 0.01; ***, P < 0.001 compared with the control (first injection).

irrespective of the slice depth (1–22 µm), were consistently closely apposed (Fig. 9). Indeed, at this spatial resolution, the vast majority of vesicles were juxtaposed to ER cisternae (Fig. 9, inset), possibly reflecting vesicle tethering in order to maintain acidic vesicle–ER junctions (Kilpatrick et al., 2012; Patel and Brailoiu, 2012).

Discussion

The current anterograde model of NAADP signaling describes acidic Ca^{2+} stores as the providers of local, trigger Ca^{2+}, which is amplified by Ca^{2+}-sensitive ER Ca^{2+} channels, IP_3Rs, or RyRs (channel chatter; Patel et al., 2001; G. Brailoiu et al., 2009;

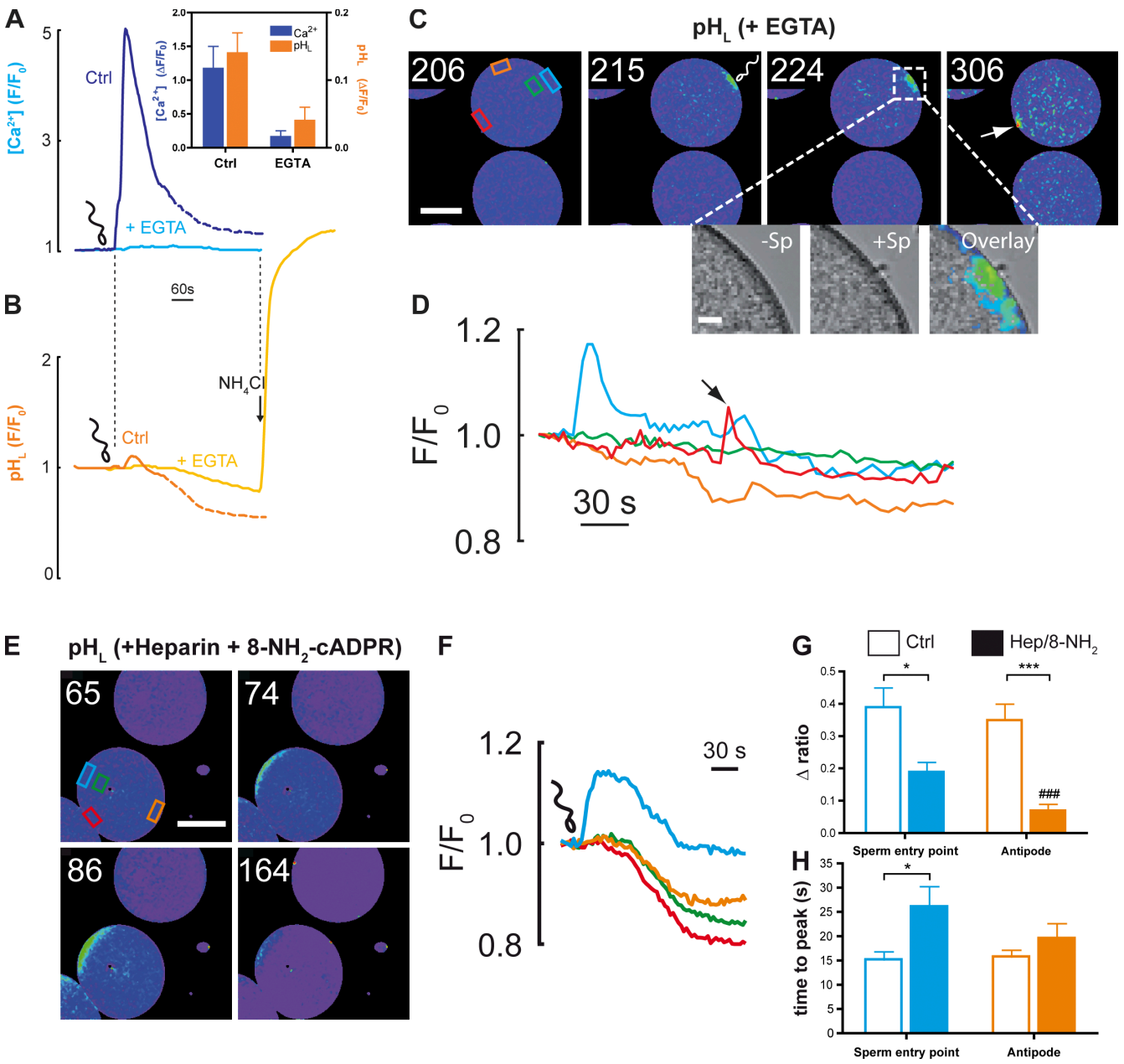

Figure 8. **Effect of inhibiting ER Ca^{2+} signaling upon the fertilization-induced pH_L changes.** (A–D) Effect of cytosolic EGTA upon Ca^{2+} and pH_L. Micropipettes containing 1 mM rhod-dextran ± 250 mM EGTA were used to inject eggs loaded with 1 µM Acridine orange. (A) Fertilization-induced peripheral Ca^{2+} responses in the absence (dark blue) or presence (light blue) of EGTA. (B) Peripheral pH_L changes in single eggs were recorded in the absence (dark orange) or presence (light orange) of EGTA. Dotted parts of the traces indicate artifacts due to changes in shape. The inset in A is a summary of 11–15 eggs. (C) Localized pH_L responses in a single EGTA-injected egg (n = 3). Images are pseudocolored F/F_0 ratios of the Acridine orange fluorescence (time in seconds) in response to sperm added at 78 s. Bottom brightfield images depict the sperm entry point at the region contained within the dotted box. The local pH_L change is overlayed. −Sp, minus sperm; +Sp, plus sperm. Bars: (main panels) 50 µm; (magnified) 10 µm. (D) Fluorescence changes at the color-matched ROIs depicted on the first image in C. The arrow in both C and D indicates the point of a second local response. (E–H) Effect of ER Ca^{2+} channel blockade upon fertilization-induced pH_L responses. Eggs were injected with or without heparin plus 8-NH_2-cADPR (500 mg/ml and 500 µM pipette concentration, respectively). (E) Pseudocolored Acridine orange F/F_0 images with time in seconds (sperm were added at 53 s). (F) Fluorescence traces from the ROIs drawn in E. Summary of the peripheral pH_L responses at the sperm entry point and antipode plotting the amplitude (G) and kinetics (H). Data represent the mean ± SEM of 11–13 eggs.

Morgan et al., 2011). Indeed, in the sea urchin egg, NAADP couples to either channel family (Churchill and Galione, 2000, 2001), hinting at a close apposition of all three channels that is made possible by the structural intimacy of the ER and acidic vesicles observed by either light (Davis et al., 2008; Morgan, 2011) or electron microscopy (Sardet, 1984; Poenie and Epel, 1987; Henson et al., 1989; Fishkind et al., 1990; McPherson et al., 1992). With such a functional triad, we wondered whether channel chatter is a two-way conversation with the ER signaling in a retrograde manner back to the acidic vesicle.

Therefore, we used pH_L as a marker of acidic store activation by NAADP. By uncaging NAADP, we verified that pH_L

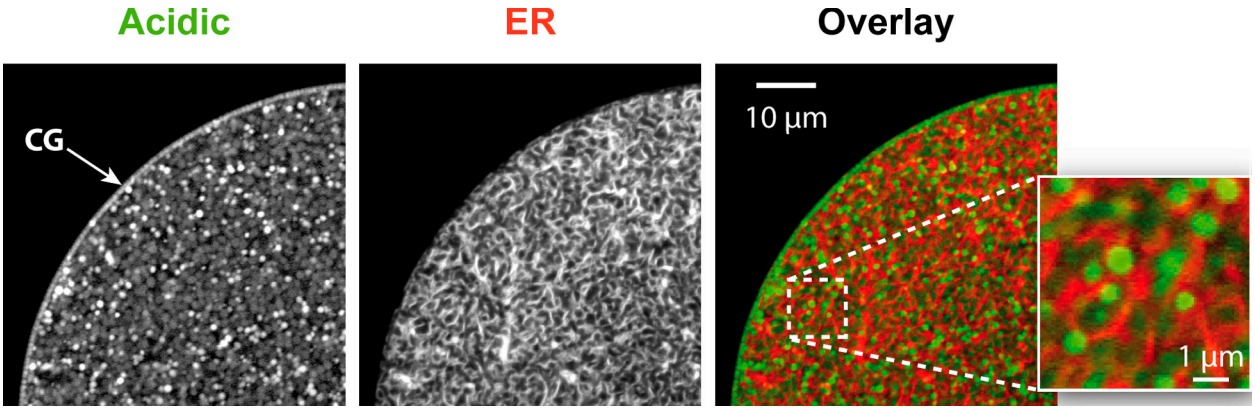

Figure 9. **Localization of acidic vesicles and ER.** Acidic vesicles were labeled with LysoTracker green and the ER with microinjected DiI and consecutive 1-µm slices were collected in an egg quarter. An equatorial slice is shown, with an arc of exocytotic cortical granules (CG) docked at the plasma membrane. Deeper vesicles show close apposition with the ER (inset). Images are representative of at least 10 eggs.

responds over an appropriate, quasi-linear concentration range and is rapid, spatially sensitive and is not distorted by diffusion. Importantly, NAADP is unique in directly activating acidic vesicles because the alkalinization in egg homogenate cannot be recapitulated by ER Ca^{2+} release agents (IP_3, cADPR, ionomycin, or SERCA inhibition; Morgan and Galione, 2007b). Finally, we verify that fertilization-induced pH_L changes are primarily dependent upon the NAADP pathway (Morgan and Galione, 2007a) judging by the effect of four NAADP inhibitors. pH_L therefore bears all the requisite hallmarks of an NAADP/acidic store reporter.

Ca^{2+} release from the ER recruits the NAADP pathway

Our primary hypothesis was that Ca^{2+} release from the ER resulted in acidic vesicle activation, and it was supported by several lines of evidence. First, the Ca^{2+} and pH_L responses mirror each other in space (see the focal photolysis of caged NAADP, sperm-induced waves, or uniform ionomycin-induced responses). Second, Ca^{2+} precedes pH_L with sperm (Morgan and Galione, 2007a) or ionomycin. Third, releasing Ca^{2+} from the ER (with ionomycin, CPA, IP_3, or cADPR) can drive a pH_LASH. Fourth, inhibiting a rise of Ca^{2+} (with Ca^{2+} buffers or intracellular channel antagonists) abrogates the pH_LASH.

In terms of the underlying pathway, we conclude that NAADP is an obligate component because the pH_LASH was blocked by NAADP antagonism or desensitization, irrespective of the ER stimulus (ionophore, second messenger, fertilization). We are confident that the antagonist pharmacology is reliable because: (1) five structurally unrelated inhibitors inhibit the pH_LASH; (2) these inhibitors are selective for the pH_LASH over the NAADP-independent central acidification; (3) they are weak inhibitors of Ca^{2+} release evoked by IP_3 or cADPR (Genazzani et al., 1997; Mándi et al., 2006; Zhang and Li, 2007; Naylor et al., 2009) or Ca^{2+}-dependent exocytosis of the fertilization envelope; (4) NAADP desensitization mimicked NAADP antagonism; and (5) pH_LASH blockade is independent of effects upon plasma membrane Ca^{2+} channels or basal pH_L. But how does ER Ca^{2+} activate acidic stores? We propose that there are two Ca^{2+}-dependent processes that can contribute to the pH_LASH—one drives NAADP synthesis, the second facilitates NAADP receptor (TPC) activation—and we shall discuss the evidence.

Ca^{2+}-dependent NAADP synthesis

The most direct evidence for Ca^{2+}-dependent NAADP synthesis was that ionomycin stimulated NAADP levels in egg populations and, correspondingly, the ionomycin-evoked pH_LASH was kinetically sluggish (consistent with the time to generate NAADP) and sensitive to NAADP antagonism. Unfortunately, we are prevented from directly testing the importance of Ca^{2+} during fertilization because *L. pictus* eggs possess low esterase activity, which precludes EGTA/AM-loading in the NAADP radioreceptor assay (Morgan and Galione, 2008). Ca^{2+}-dependent messenger production has precedents in IP_3 (Thaler et al., 2004), cADPR (Kim et al., 2008; Shawl et al., 2009), and cAMP (Cooper, 2003) and is an emerging theme for NAADP too, having been postulated in sperm (Vasudevan et al., 2010). At present we cannot say whether Ca^{2+} is the sole stimulus of NAADP synthesis at fertilization, but it suggests that Ca^{2+} can be a component.

Ca^{2+} feedback at NAADP-sensitive channels

Nevertheless, NAADP synthesis cannot readily explain all aspects of the Ca^{2+}-dependent activation of acidic vesicles. For instance, the slow kinetics (≤70 s) of the ionomycin-induced pH_LASH are credibly consistent with synthesis, but the more rapid effects of IP_3 or cADPR (≤4 s) are more difficult to rationalize in such terms (unless exquisitely coupled). We therefore invoke a direct action of Ca^{2+} upon the acidic stores themselves.

First, for acidic vesicle activation, NAADP exhibited a co-requirement for Ca^{2+} because the pH_LASH was sensitive to Ca^{2+} chelators, EGTA and BAPTA. Moreover, the degree of inhibition was commensurate with the kinetics of Ca^{2+} buffering (slow EGTA was weaker than was fast BAPTA). With ∼2.5 mM chelator in the cytosol, one can calculate (Stern, 1992; Dargan and Parker, 2003 [assuming a 200 $\mu m^2/s$ Ca^{2+} diffusion coefficient appropriate for high concentrations of Ca^{2+} around a channel; Allbritton et al., 1992; Naraghi and Neher, 1997]) that the maximum range of Ca^{2+} action after release from a channel would be ∼300 nm in the presence of EGTA but ∼10 nm in the presence

of BAPTA. In other words, the Ca^{2+} released by NAADP must be acting locally in microdomains 10–300 nm from the TPC to facilitate the pH_{LASH} (compare microdomains in other systems; G. Brailoiu et al., 2009). Given that Ca^{2+} channel complexes span 15–28 nm in diameter (Samsó and Wagenknecht, 1998; Wolf et al., 2003; Taylor et al., 2004), we propose that Ca^{2+} feedback reinforces TPC activation at the intra- as well as intermolecular level.

Acidic vesicle/ER junctions

It is this Ca^{2+} sensitivity of the NAADP system that may partly explain the trans-stimulation of acidic stores by Ca^{2+} from the ER. The NAADP-induced pH_{LASH} was robust in the presence of EGTA, indicating that TPC activation remained detectable. Nonetheless, the pH_{LASH} evoked by IP_3 or cADPR was completely blocked by EGTA pointing to the coupling mechanism being affected. The effect of EGTA is unlikely to be due to simply blocking Ca^{2+} release at IP_3Rs/RyRs because local CICR and ER channel opening persist in the presence of the slow chelator (Dargan and Parker, 2003; Dargan et al., 2004; Shuai and Parker, 2005; Smith and Parker, 2009). We conclude that EGTA prevents a pH_{LASH} by buffering the ER Ca^{2+} within the junction before it reaches target sites on adjacent vesicles.

Our staining of the ER and acidic vesicles revealed a close proximity, and electron micrographs of the sea urchin egg cortex confirm the close (≤300 nm) apposition of acidic vesicles and ER elements (Sardet, 1984; Poenie and Epel, 1987; Henson et al., 1989; Fishkind et al., 1990; McPherson et al., 1992). Nevertheless, our functional data suggest that the resident IP_3Rs and RyRs, though close, must be farther than 300 nm from the Ca^{2+}-sensitive targets in order to be EGTA sensitive. This can be rationalized if the channels are slightly along the ER branches and RyR immunogold labeling is consistent with such distances (McPherson et al., 1992), but comparable data for IP_3Rs are not available. A preferential closeness of RyRs and TPCs is feasible because RyRs (McPherson et al., 1992) and TPCs (Ruas et al., 2010) are relatively denser in the cortical (i.e., pH_{LASH}) region compared with IP_3Rs (Parys et al., 1994). In addition, the larger Ca^{2+} conductance of RyRs compared with IP_3Rs (Pitt et al., 2010) might also contribute to preferential coupling. Such communication between ER and acidic vesicles is lost upon homogenization (Morgan and Galione, 2007b), conceivably because it destroys the native apposition of the two organelles.

Given the inhibition by NAADP antagonism/desensitization, ER Ca^{2+} appears to stimulate TPCs on the acidic vesicles. Considering that cytosolic Ca^{2+} effects at the NAADP receptor have hitherto been discounted (Chini and Dousa, 1996; Genazzani and Galione, 1996; Bak et al., 1999; Mándi et al., 2006), such a Ca^{2+} stimulation may instead occur at the luminal face of NAADP-regulated channels (after Ca^{2+} uptake): high luminal [Ca^{2+}] appears to enhance the conductance of sea urchin NAADP receptors (Morgan et al., 2012), TPC1 (Rybalchenko et al., 2012) and TPC2 (Pitt et al., 2010), analogous to the luminal regulation of IP_3Rs and RyRs (Burdakov et al., 2005). Ca^{2+} transfer from ER to acidic vesicles would be reminiscent of bidirectional communication between other inter-organelle partnerships such as ER/mitochondria (Arnaudeau et al., 2001; Rizzuto and Pozzan, 2006).

Bidirectional signaling during cell stimulation

Is retrograde signaling from ER to acidic vesicle physiological? NAADP antagonism confirmed that the fertilization-induced pH_{LASH} is driven primarily by NAADP (Morgan and Galione, 2007a), but the fact that Ca^{2+} chelation and ER channel blockers also inhibit the pH_{LASH} at fertilization points to an additional role of cADPR/IP_3. In particular, this blockade of the ER "balkanizes" the pH_{LASH} around the sperm entry site and is consistent with the retrograde signal amplifying acidic store activation.

What might be the order of events at fertilization? When a sperm contacts the egg jelly, NAADP first rapidly increases within the sperm head (Churchill et al., 2003) to drive the acrosome reaction (Vasudevan et al., 2010) and, incidentally, to provide a preformed bolus of NAADP that can be delivered to the egg upon fusion (Churchill et al., 2003). In the absence of egg amplification (i.e., plus EGTA or ER channel blockade), the early focal pH_L change around the sperm entry point is certainly consistent with a visualization of this NAADP delivery.

Because the volume of the sperm is ∼6 orders of magnitude smaller than the egg's, dilution of the bolus in the vast egg cytosol necessitates further NAADP production within the egg. We therefore propose that the observed slow second phase of NAADP synthesis (Churchill et al., 2003) can be driven by an increase in Ca^{2+} that is dependent upon cADPR/IP_3; this is analogous to waves of IP_3 synthesis stimulated by Ca^{2+} in sea urchin eggs (Kuroda et al., 2001; Thaler et al., 2004).

If cADPR and IP_3 provide ER Ca^{2+} to facilitate the NAADP pathway, then these ER messengers should precede the second (egg) phase of NAADP synthesis (Churchill et al., 2003); their involvement in the initiation and propagation of the fertilization Ca^{2+} wave (Galione et al., 1993; Lee et al., 1993; Davis et al., 2008) and the kinetics of cADPR or IP_3 production (Kuroda et al., 2001; Leckie et al., 2003; Thaler et al., 2004) favor this idea.

In addition to this novel retrograde signaling mode, conventional anterograde signals from the acidic vesicles to the ER do occur in the egg: NAADP-induced Ca^{2+} release recruits cADPR and IP_3, as expected (Churchill and Galione, 2000). Hence, we envisage mutually supportive Ca^{2+} feedback between acidic vesicles and ER as the Ca^{2+} wave front propagates across the egg.

Beyond the egg

Our current work expands the channel chatter model into a two-way conversation between ER and acidic Ca^{2+} stores. Reports of NAADP acting downstream of IP_3 or cADPR are few and have not detailed a mechanism (e.g., in ascidian oocytes [Albrieux et al., 1998] and T-lymphocytes [Berg et al., 2000]), but the implications may be far reaching: we do not understand how NAADP is choreographed during Ca^{2+} oscillations and waves in mammalian cells, in spite of its importance (Cancela et al., 1999). Our model provides a reinforcement loop whereby consecutive rounds of acidic vesicle-to-ER and ER-to-acidic vesicle Ca^{2+} feedback occur during oscillations, e.g., during the pacemaker rise of the next spike or at the Ca^{2+} wave front (Fig. S4). Local ER/acidic vesicle communication has also been highlighted recently in mammalian cells (Kilpatrick et al., 2012;

Sanjurjo et al., 2012). That the ER can signal to acidic vesicles may also have far-reaching implications for endo-lysosomal functions such as resident enzyme activity, autophagy, and the pathology of diseases that affect lysosomal Ca^{2+} fluxes (Lloyd-Evans et al., 2008; Morgan et al., 2011; Coen et al., 2012).

Materials and methods

Gamete preparation

Sea urchin eggs from *Lytechinus pictus* were harvested by intracoelomic injection of 0.5 M KCl and collected in artificial sea water (ASW [mM]: 435 NaCl, 40 $MgCl_2$, 15 $MgSO_4$, 11 $CaCl_2$, 10 KCl, 2.5 $NaHCO_3$, and 20 Tris, pH 8.0), and de-jellied by passage through 100-µm nylon mesh (EMD Millipore). Sperm, on the other hand, were collected "dry" and maintained at 4°C until use.

Confocal laser scanning microscopy

Eggs were maintained at room temperature in ASW and imaged on glass poly-D-lysine–coated coverslips mounted on a confocal laser scanning microscope (LSM 510 Meta; Carl Zeiss); an Axiovert 200M (Carl Zeiss) equipped with Zeiss objectives (10× Neofluar, NA 0.3; 40× Fluar, NA 1.3) was controlled by LSM software (Carl Zeiss). Excitation/emission (nm) wavelengths per channel were 351/>385 (UV), 488/505–530 (green), 543/>560 (red), 633/645–719 (far-red). When inhibitors were tested at fertilization, eggs were preincubated with the inhibitors (or vehicle) but sperm were preactivated in ASW without inhibitors for 20–30 s before their addition to eggs in order to minimize drug effects upon sperm. Images were analyzed using custom-written Magipix software (R. Jacob, King's College London, London, England, UK).

pH_L and Ca^{2+} measurements

pH_L was usually monitored ratiometrically in eggs co-loaded with 10 µM Acridine orange and 1 µM LysoTracker red DND-99 for 15–20 min at room temperature and imaged using green/red channels, respectively, as described previously (Morgan and Galione, 2007a). Data are expressed as the ratio of the Acridine orange/LysoTracker red signals with an increase in the ratio reflecting an increase in pH_L.

In pH_L experiments where different second messengers were consecutively injected, eggs were labeled with 10 µM Acridine orange only (10–30 min) and its fluorescence monitored simultaneously with that of the injection marker (see following section). Because of the slight change of cell shape elicited by the first injection (due to fertilization envelope lifting), the peripheral region of interest was always redefined to monitor the fluorescence response to the second injection.

Cytosolic Ca^{2+} was measured in two modes: ratiometric recording involved coinjecting eggs with 10 kD dextran conjugates of fluo-4 (Ca^{2+}-sensitive) and Alexa Fluor 647 (Ca^{2+}-insensitive) at pipette concentrations of 1 mM and 250 µM, respectively (data are expressed as the green/far-red ratio); alternatively, single wavelength recording used either fluo-4 dextran (green channel) or rhod-dextran (high affinity form, red channel) only.

Caged compounds and photolysis

Caged NAADP was synthesized in-house using sequential reactions (Lee et al., 1997; Morgan et al., 2006). In brief, 2-nitroacetophenone hydrazone was synthesized from 2-nitroacetophenone and hydrazine monohydrate under acidic conditions; the chloroform-extracted hydrazone was then converted to 1(2-nitrophenyl)diazoethane using MnO_2 and finally incubated with NAADP under acidic conditions to cage the phosphate groups. The caged product was purified by HPLC and stored at −80°C. After treatment with alkaline phosphatase beads (to remove contaminating free NAADP), caged NAADP was then microinjected into eggs (50-µM pipette concentration) together with 1 mM fluo-4 dextran to measure Ca^{2+} or with 50–200 µM Alexa Fluor 647 dextran as an injection marker for pH_L recordings. Photolysis was effected with a Coherent Enterprise UV laser (351 nm) and exposure was either global (70% power, 5 frames at 1 Hz) or focal (10–70% power, 2 iterations) as controlled by an acousto-optical tunable filter.

Caged Ca^{2+} (NP-EGTA) at 25 mM in 10 mM Hepes (pH 7) was coinjected with either fluo-4 dextran or Alexa Fluor 647 dextran. Focal photolysis was effected by UV laser (351- and 364-nm lines, 20 iterations at 50–75% power).

Ned-19 fluorescence

We exploited the intrinsic fluorescence of Ned-19 to monitor its loading into intact eggs (excitation at 364 nm; emission >385 nm). To minimize photobleaching, images were captured discontinuously after known times of Ned-19 preincubation and all with identical acquisition settings. We also confirmed that the fluorescence of Ned-19 did not interfere with Acridine orange fluorescence in vitro: 10 µM Acridine orange fluorescence was recorded in a fluorimeter (excitation 488 nm, emission 526 nm; model LS-50B, PerkinElmer) in a medium containing (mM): 250 potassium gluconate, 250 *N*-methylglucamine, 20 Hepes, and 1 $MgCl_2$, pH 5.5. In the presence of 100 and 200 µM Ned-19, the Acridine orange signal was 106 ± 2 and 109 ± 3% of that in the absence of Ned-19, respectively (n = 3, $P > 0.1$).

Organelle localization

Labeling of ER and acidic vesicles was performed as described previously (Terasaki and Jaffe, 1991; Davis et al., 2008). In summary, a saturated solution of DiI ($DiIC_{18}$(3)) was prepared by vortexing a few grains of DiI in 200 µl of soybean oil and was microinjected into the egg center. The DiI diffused from the central oil droplet into the contiguous membrane system of the ER in 15–30 min, during which time acidic vesicles were labeled by addition of 1 µM LysoTracker green DND-26 (Invitrogen). Confocal 1-µm optical sections were collected using the standard green and red channel settings.

NAADP levels

For the NAADP assay, NAADP and [^{32}P]NAADP were enzymatically synthesized in-house using the base-exchange reaction of Aplysia ADP-ribosyl cyclase (ARC; Lee et al., 1997; Morgan et al., 2006; Vasudevan et al., 2010). For NAADP, 13 mM NADP and 100 mM nicotinic acid were incubated at pH 4.5 with ARC for 1 h at room temperature and NAADP purified by HPLC. Two stages were required for [^{32}P]NAADP: first, [^{32}P]NAD was phosphorylated to [^{32}P]NADP using human NAD kinase and 10 mM ATP; second, the product was converted to [^{32}P]NAADP by incubating with 100 mM nicotinic acid and ARC at pH 4.5 for 1 h at room temperature, and purified by HPLC.

The time course of NAADP changes in populations of eggs stimulated with sperm or ionomycin was determined biochemically. For a given experiment, 1 ml of eggs was diluted into 20 ml of ASW. A 2-ml aliquot was taken from this solution at each time point and centrifuged at 9,000 *g*. Centrifugation was then stopped as swiftly as possible, and the supernatant discarded. 100 µl $HClO_4$ was then added. To disrupt the cells, sonication was performed (Jencons Vibra-Cell at amplitude 60) for three bursts of 5 s. The time point was taken as the start of sonication and samples were then placed on ice. The denatured protein was pelleted by centrifugation at 9,000 *g* for 10 min and stored at −80°C for later analysis. The supernatant was neutralized with an equal volume of 2 M $KHCO_3$ and vortexed. Centrifugation at 9,000 *g* for 10 min was again used to remove the $KClO_4$ precipitate. The resulting supernatant was stored at −80°C for NAADP analysis. The protein concentration in the precipitated pellet was determined using the BCA reagent.

As reported in detail previously (Lewis et al., 2007), NAADP levels were determined using the NAADP-binding protein from sea urchin (*L. pictus*) egg homogenate, which is highly selective for NAADP (Churamani et al., 2004; Lewis et al., 2007). First, we added 25 µl of test sample to each tube and then added 125 µl of 1% (vol/vol) sea urchin egg homogenate in intracellular medium and incubated the reaction for 10 min at 25°C. To each tube we then added 0.2 nM of [^{32}P]NAADP (~50,000 cpm) diluted in 100 µl of intracellular medium (250 mM *N*-methyl-D-glucamine, 250 mM potassium gluconate, 1 mM $MgCl_2$, and 20 mM Hepes, pH 7.2) and incubated the reaction for 10 min at 25°C. Bound NAADP was then trapped onto Whatman GF/B filter papers using a Brandel cell harvester. We washed the filters three times with 1 ml of a buffer containing 20 mM Hepes and 500 mM potassium acetate, pH 7.4, and the bound radioactivity was estimated by phosphorimaging. The amount of NAADP in each test sample was determined by comparison with a standard curve containing known amounts of NAADP. Results are normalized to the protein content (pmol NAADP/mg protein).

Statistical analysis

Fluorescence traces in all figures are from single cells representative of n eggs from ≥3 preparations unless indicated otherwise. Data are expressed as the mean ± SEM. Two datasets were compared using Student's t test, whereas multiple groups were analyzed using ANOVA and a Tukey-Kramer or Dunnett's post-test. A nonparametric ANOVA (Kruskal-Wallis and Dunn post-test) was applied when required. Data were paired where appropriate and significance assumed at $P < 0.05$.

Reagents

Caged NAADP, free NAADP, and [^{32}P]NAADP were synthesized in-house. [^{32}P]β-NAD^+ was obtained from GE Healthcare. IP_3 was from LC Laboratories.

Cyclic ADP-ribose, NAADP, IP_3, PPADS (pyridoxalphosphate-6-azophenyl-2′4′-disulfonic acid), EGTA, BAPTA, heparin (low MW), 8-NH_2-cADPR, diltiazem, nifedipine, cyclopiazonic acid, ADP-ribosyl cyclase, and soybean oil were obtained from Sigma-Aldrich. Ned-19 (mixed isomers) was from IBScreen (Moscow, Russia). Acridine orange, LysoTracker red DND-99, rhod-dextran (10 kD, high affinity form), Fluo-4 dextran (10 kD), Alexa Fluor 647 dextran (10 kD), NP-EGTA (potassium salt), and $DiIC_{18}(3)$ were from Invitrogen. Ionomycin and SKF96365 were from EMD Millipore. NAD kinase was a kind gift from M. Ziegler (University of Bergen, Bergen, Norway). All other reagents were of analytical grade.

Online supplemental material

Fig. S1 shows the regenerative propagation of the pH_L response away from the focal photolysis region in a minority of eggs and compares such real responses with theoretical models. Fig. S2 compares the effect of NAADP antagonists upon Ca^{2+} release in egg homogenate evoked by NAADP, cADPR, and IP_3; the effect of removing extracellular Ca^{2+} on the pH_{LASH} in intact eggs is also shown. Fig. S3 shows that cADPR-induced Ca^{2+} release in intact eggs is desensitized by prior injection of NAADP. Fig. S4 is a scheme summarizing how Ca^{2+} from the ER may stimulate the NAADP pathway in eggs and mammalian cells. Online supplemental material is available at http://www.jcb.org/cgi/content/full/jcb.201204078/DC1.

We thank Clive Garnham for technical assistance, Margarida Ruas for invaluable suggestions, and the Wellcome Trust for financial support.

There are no conflicts of interest.

Submitted: 16 April 2012
Accepted: 12 February 2013

References

Albrieux, M., H.C. Lee, and M. Villaz. 1998. Calcium signaling by cyclic ADP-ribose, NAADP, and inositol trisphosphate are involved in distinct functions in ascidian oocytes. *J. Biol. Chem.* 273:14566–14574. http://dx.doi.org/10.1074/jbc.273.23.14566

Allbritton, N.L., T. Meyer, and L. Stryer. 1992. Range of messenger action of calcium ion and inositol 1,4,5-trisphosphate. *Science*. 258:1812–1815. http://dx.doi.org/10.1126/science.1465619

Arnaudeau, S., W.L. Kelley, J.V. Walsh Jr., and N. Demaurex. 2001. Mitochondria recycle Ca^{2+} to the endoplasmic reticulum and prevent the depletion of neighboring endoplasmic reticulum regions. *J. Biol. Chem.* 276:29430–29439. http://dx.doi.org/10.1074/jbc.M103274200

Bak, J., P. White, G. Timár, L. Missiaen, A.A. Genazzani, and A. Galione. 1999. Nicotinic acid adenine dinucleotide phosphate triggers Ca^{2+} release from brain microsomes. *Curr. Biol.* 9:751–754. http://dx.doi.org/10.1016/S0960-9822(99)80335-2

Barceló-Torns, M., A.M. Lewis, A. Gubern, D. Barneda, D. Bloor-Young, F. Picatoste, G.C. Churchill, E. Claro, and R. Masgrau. 2011. NAADP mediates ATP-induced Ca^{2+} signals in astrocytes. *FEBS Lett.* 585:2300–2306. http://dx.doi.org/10.1016/j.febslet.2011.05.062

Berg, I., B.V. Potter, G.W. Mayr, and A.H. Guse. 2000. Nicotinic acid adenine dinucleotide phosphate ($NAADP^+$) is an essential regulator of T-lymphocyte Ca^{2+}-signaling. *J. Cell Biol.* 150:581–588. http://dx.doi.org/10.1083/jcb.150.3.581

Berridge, M.J., M.D. Bootman, and H.L. Roderick. 2003. Calcium signalling: dynamics, homeostasis and remodelling. *Nat. Rev. Mol. Cell Biol.* 4:517–529. http://dx.doi.org/10.1038/nrm1155

Bezin, S., G. Charpentier, H.C. Lee, G. Baux, P. Fossier, and J.M. Cancela. 2008. Regulation of nuclear Ca^{2+} signaling by translocation of the Ca^{2+} messenger synthesizing enzyme ADP-ribosyl cyclase during neuronal depolarization. *J. Biol. Chem.* 283:27859–27870. http://dx.doi.org/10.1074/jbc.M804701200

Billington, R.A., and A.A. Genazzani. 2007. PPADS is a reversible competitive antagonist of the NAADP receptor. *Cell Calcium*. 41:505–511. http://dx.doi.org/10.1016/j.ceca.2006.10.002

Brailoiu, E., D. Churamani, X. Cai, M.G. Schrlau, G.C. Brailoiu, X. Gao, R. Hooper, M.J. Boulware, N.J. Dun, J.S. Marchant, and S. Patel. 2009. Essential requirement for two-pore channel 1 in NAADP-mediated calcium signaling. *J. Cell Biol.* 186:201–209. http://dx.doi.org/10.1083/jcb.200904073

Brailoiu, E., R. Hooper, X. Cai, G.C. Brailoiu, M.V. Keebler, N.J. Dun, J.S. Marchant, and S. Patel. 2010a. An ancestral deuterostome family of two-pore channels mediates nicotinic acid adenine dinucleotide phosphate-dependent calcium release from acidic organelles. *J. Biol. Chem.* 285:2897–2901. http://dx.doi.org/10.1074/jbc.C109.081943

Brailoiu, E., T. Rahman, D. Churamani, D.L. Prole, G.C. Brailoiu, R. Hooper, C.W. Taylor, and S. Patel. 2010b. An NAADP-gated two-pore channel targeted to the plasma membrane uncouples triggering from amplifying Ca^{2+} signals. *J. Biol. Chem.* 285:38511–38516. http://dx.doi.org/10.1074/jbc.M110.162073

Brailoiu, G.C., E. Brailoiu, R. Parkesh, A. Galione, G.C. Churchill, S. Patel, and N.J. Dun. 2009. NAADP-mediated channel 'chatter' in neurons of the rat medulla oblongata. *Biochem. J.* 419:91–97: 2: 97. http://dx.doi.org/10.1042/BJ20081138

Burdakov, D., O.H. Petersen, and A. Verkhratsky. 2005. Intraluminal calcium as a primary regulator of endoplasmic reticulum function. *Cell Calcium*. 38:303–310. http://dx.doi.org/10.1016/j.ceca.2005.06.010

Calcraft, P.J., M. Ruas, Z. Pan, X. Cheng, A. Arredouani, X. Hao, J. Tang, K. Rietdorf, L. Teboul, K.T. Chuang, et al. 2009. NAADP mobilizes calcium from acidic organelles through two-pore channels. *Nature*. 459:596–600. http://dx.doi.org/10.1038/nature08030

Cancela, J.M., G.C. Churchill, and A. Galione. 1999. Coordination of agonist-induced Ca^{2+}-signalling patterns by NAADP in pancreatic acinar cells. *Nature*. 398:74–76. http://dx.doi.org/10.1038/18032

Cancela, J.M., F. Van Coppenolle, A. Galione, A.V. Tepikin, and O.H. Petersen. 2002. Transformation of local Ca^{2+} spikes to global Ca^{2+} transients: the combinatorial roles of multiple Ca^{2+} releasing messengers. *EMBO J.* 21:909–919. http://dx.doi.org/10.1093/emboj/21.5.909

Chini, E.N., and T.P. Dousa. 1996. Nicotinate-adenine dinucleotide phosphate-induced Ca^{2+}-release does not behave as a Ca^{2+}-induced Ca^{2+}-release system. *Biochem. J.* 316:709–711.

Churamani, D., E.A. Carrey, G.D. Dickinson, and S. Patel. 2004. Determination of cellular nicotinic acid-adenine dinucleotide phosphate (NAADP) levels. *Biochem. J.* 380:449–454. http://dx.doi.org/10.1042/BJ20031754

Churchill, G.C., and A. Galione. 2000. Spatial control of Ca^{2+} signaling by nicotinic acid adenine dinucleotide phosphate diffusion and gradients. *J. Biol. Chem.* 275:38687–38692. http://dx.doi.org/10.1074/jbc.M005827200

Churchill, G.C., and A. Galione. 2001. NAADP induces Ca^{2+} oscillations via a two-pool mechanism by priming IP_3- and cADPR-sensitive Ca^{2+} stores. *EMBO J.* 20:2666–2671. http://dx.doi.org/10.1093/emboj/20.11.2666

Churchill, G.C., Y. Okada, J.M. Thomas, A.A. Genazzani, S. Patel, and A. Galione. 2002. NAADP mobilizes Ca^{2+} from reserve granules, lysosome-related organelles, in sea urchin eggs. *Cell*. 111:703–708. http://dx.doi.org/10.1016/S0092-8674(02)01082-6

Churchill, G.C., J.S. O'Neill, R. Masgrau, S. Patel, J.M. Thomas, A.A. Genazzani, and A. Galione. 2003. Sperm deliver a new second messenger: NAADP. *Curr. Biol.* 13:125–128. http://dx.doi.org/10.1016/S0960-9822(03)00002-2

Coen, K., R.S. Flannagan, S. Baron, L.R. Carraro-Lacroix, D. Wang, W. Vermeire, C. Michiels, S. Munck, V. Baert, S. Sugita, et al. 2012. Lysosomal calcium homeostasis defects, not proton pump defects, cause endo-lysosomal dysfunction in PSEN-deficient cells. *J. Cell Biol.* 198:23–35. http://dx.doi.org/10.1083/jcb.201201076

Collins, T.P., R. Bayliss, G.C. Churchill, A. Galione, and D.A. Terrar. 2011. NAADP influences excitation-contraction coupling by releasing calcium from lysosomes in atrial myocytes. *Cell Calcium*. 50:449–458. http://dx.doi.org/10.1016/j.ceca.2011.07.007

Cooper, D.M. 2003. Regulation and organization of adenylyl cyclases and cAMP. *Biochem. J.* 375:517–529. http://dx.doi.org/10.1042/BJ20031061

Cosker, F., N. Cheviron, M. Yamasaki, A. Menteyne, F.E. Lund, M.J. Moutin, A. Galione, and J.M. Cancela. 2010. The ecto-enzyme CD38 is a nicotinic acid adenine dinucleotide phosphate (NAADP) synthase that couples receptor activation to Ca^{2+} mobilization from lysosomes in pancreatic acinarcells. *J. Biol. Chem.* 285:38251–38259. http://dx.doi.org/10.1074/jbc.M110.125864

Dargan, S.L., and I. Parker. 2003. Buffer kinetics shape the spatiotemporal patterns of IP_3-evoked Ca^{2+} signals. *J. Physiol.* 553:775–788. http://dx.doi.org/10.1113/jphysiol.2003.054247

Dargan, S.L., B. Schwaller, and I. Parker. 2004. Spatiotemporal patterning of IP_3-mediated Ca^{2+} signals in *Xenopus* oocytes by Ca^{2+}-binding proteins. *J. Physiol.* 556:447–461. http://dx.doi.org/10.1113/jphysiol.2003.059204

Davis, L.C., A.J. Morgan, M. Ruas, J.L. Wong, R.M. Graeff, A.J. Poustka, H.C. Lee, G.M. Wessel, J. Parrington, and A. Galione. 2008. Ca^{2+} signaling occurs via second messenger release from intraorganelle synthesis sites. *Curr. Biol.* 18:1612–1618. http://dx.doi.org/10.1016/j.cub.2008.09.024

Davis, L.C., A.J. Morgan, J.L. Chen, C.M. Snead, D. Bloor-Young, E. Shenderov, M.N. Stanton-Humphreys, S.J. Conway, G.C. Churchill, J. Parrington, et al. 2012. NAADP activates two-pore channels on T cell cytolytic granules to stimulate exocytosis and killing. *Curr. Biol.* 22:1–7. http://dx.doi.org/10.1016/j.cub.2012.10.035

Fasolato, C., M. Zottini, E. Clementi, D. Zacchetti, J. Meldolesi, and T. Pozzan. 1991. Intracellular Ca^{2+} pools in PC12 cells. Three intracellular pools are

distinguished by their turnover and mechanisms of Ca^{2+} accumulation, storage, and release. *J. Biol. Chem.* 266:20159–20167.

Fishkind, D.J., E.M. Bonder, and D.A. Begg. 1990. Subcellular localization of sea urchin egg spectrin: evidence for assembly of the membrane-skeleton on unique classes of vesicles in eggs and embryos. *Dev. Biol.* 142:439–452. http://dx.doi.org/10.1016/0012-1606(90)90366-Q

Galione, A., A. McDougall, W.B. Busa, N. Willmott, I. Gillot, and M. Whitaker. 1993. Redundant mechanisms of calcium-induced calcium release underlying calcium waves during fertilization of sea urchin eggs. *Science*. 261:348–352. http://dx.doi.org/10.1126/science.8392748

Genazzani, A.A., and A. Galione. 1996. Nicotinic acid-adenine dinucleotide phosphate mobilizes Ca^{2+} from a thapsigargin-insensitive pool. *Biochem. J.* 315:721–725.

Genazzani, A.A., M. Mezna, D.M. Dickey, F. Michelangeli, T.F. Walseth, and A. Galione. 1997. Pharmacological properties of the Ca^{2+}-release mechanism sensitive to NAADP in the sea urchin egg. *Br. J. Pharmacol.* 121:1489–1495. http://dx.doi.org/10.1038/sj.bjp.0701295

Henson, J.H., D.A. Begg, S.M. Beaulieu, D.J. Fishkind, E.M. Bonder, M. Terasaki, D. Lebeche, and B. Kaminer. 1989. A calsequestrin-like protein in the endoplasmic reticulum of the sea urchin: localization and dynamics in the egg and first cell cycle embryo. *J. Cell Biol.* 109:149–161. http://dx.doi.org/10.1083/jcb.109.1.149

Hirohashi, N., and V.D. Vacquier. 2003. Store-operated calcium channels trigger exocytosis of the sea urchin sperm acrosomal vesicle. *Biochem. Biophys. Res. Commun.* 304:285–292. http://dx.doi.org/10.1016/S0006-291X(03)00587-4

Kidd, J.F., K.E. Fogarty, R.A. Tuft, and P. Thorn. 1999. The role of Ca^{2+} feedback in shaping $InsP_3$-evoked Ca^{2+} signals in mouse pancreatic acinar cells. *J. Physiol.* 520:187–201. http://dx.doi.org/10.1111/j.1469-7793.1999.00187.x

Kilpatrick, B.S., E.R. Eden, A.H. Schapira, C.E. Futter, and S. Patel. 2012. Direct mobilisation of lysosomal Ca^{2+} triggers complex Ca^{2+} signals. *J. Cell Sci.* http://dx.doi.org/ 10.1242/jcs.118836

Kim, B.J., K.H. Park, C.Y. Yim, S. Takasawa, H. Okamoto, M.J. Im, and U.H. Kim. 2008. Generation of nicotinic acid adenine dinucleotide phosphate and cyclic ADP-ribose by glucagon-like peptide-1 evokes Ca^{2+} signal that is essential for insulin secretion in mouse pancreatic islets. *Diabetes*. 57:868–878. http://dx.doi.org/10.2337/db07-0443

Kinnear, N.P., F.X. Boittin, J.M. Thomas, A. Galione, and A.M. Evans. 2004. Lysosome-sarcoplasmic reticulum junctions. A trigger zone for calcium signaling by nicotinic acid adenine dinucleotide phosphate and endothelin-1. *J. Biol. Chem.* 279:54319–54326. http://dx.doi.org/10.1074/jbc.M406132200

Kuroda, R., K. Kontani, Y. Kanda, T. Katada, T. Nakano, Y. Satoh, N. Suzuki, and H. Kuroda. 2001. Increase of cGMP, cADP-ribose and inositol 1,4,5-trisphosphate preceding Ca^{2+} transients in fertilization of sea urchin eggs. *Development*. 128:4405–4414.

Leckie, C., R. Empson, A. Becchetti, J. Thomas, A. Galione, and M. Whitaker. 2003. The NO pathway acts late during the fertilization response in sea urchin eggs. *J. Biol. Chem.* 278:12247–12254. http://dx.doi.org/10.1074/jbc.M210770200

Lee, H.C., and D. Epel. 1983. Changes in intracellular acidic compartments in sea urchin eggs after activation. *Dev. Biol.* 98:446–454. http://dx.doi.org/10.1016/0012-1606(83)90374-3

Lee, H.C., R. Aarhus, and T.F. Walseth. 1993. Calcium mobilization by dual receptors during fertilization of sea urchin eggs. *Science*. 261:352–355. http://dx.doi.org/10.1126/science.8392749

Lee, H.C., R. Aarhus, K.R. Gee, and T. Kestner. 1997. Caged nicotinic acid adenine dinucleotide phosphate. Synthesis and use. *J. Biol. Chem.* 272:4172–4178. http://dx.doi.org/10.1074/jbc.272.7.4172

Lewis, A.M., R. Masgrau, S.R. Vasudevan, M. Yamasaki, J.S. O'Neill, C. Garnham, K. James, A. Macdonald, M. Ziegler, A. Galione, and G.C. Churchill. 2007. Refinement of a radioreceptor binding assay for nicotinic acid adenine dinucleotide phosphate. *Anal. Biochem.* 371:26–36. http://dx.doi.org/10.1016/j.ab.2007.08.030

Lloyd-Evans, E., A.J. Morgan, X. He, D.A. Smith, E. Elliot-Smith, D.J. Sillence, G.C. Churchill, E.H. Schuchman, A. Galione, and F.M. Platt. 2008. Niemann-Pick disease type C1 is a sphingosine storage disease that causes deregulation of lysosomal calcium. *Nat. Med.* 14:1247–1255. http://dx.doi.org/10.1038/nm.1876

Macgregor, A., M. Yamasaki, S. Rakovic, L. Sanders, R. Parkesh, G.C. Churchill, A. Galione, and D.A. Terrar. 2007. NAADP controls cross-talk between distinct Ca^{2+} stores in the heart. *J. Biol. Chem.* 282:15302–15311. http://dx.doi.org/10.1074/jbc.M611167200

Mándi, M., B. Tóth, G. Timár, and J. Bak. 2006. Ca^{2+} release triggered by NAADP in hepatocyte microsomes. *Biochem. J.* 395:233–238. http://dx.doi.org/10.1042/BJ20051002

McPherson, S.M., P.S. McPherson, L. Mathews, K.P. Campbell, and F.J. Longo. 1992. Cortical localization of a calcium release channel in sea urchin eggs. *J. Cell Biol.* 116:1111–1121. http://dx.doi.org/10.1083/jcb.116.5.1111

Moccia, F., D. Lim, K. Kyozuka, and L. Santella. 2004. NAADP triggers the fertilization potential in starfish oocytes. *Cell Calcium*. 36:515–524. http://dx.doi.org/10.1016/j.ceca.2004.05.004

Moccia, F., G.A. Nusco, D. Lim, K. Kyozuka, and L. Santella. 2006. NAADP and $InsP_3$ play distinct roles at fertilization in starfish oocytes. *Dev. Biol.* 294:24–38. http://dx.doi.org/10.1016/j.ydbio.2006.02.011

Morgan, A.J. 2011. Sea urchin eggs in the acid reign. *Cell Calcium*. 50:147–156. http://dx.doi.org/10.1016/j.ceca.2010.12.007

Morgan, A.J., and A. Galione. 2007a. Fertilization and nicotinic acid adenine dinucleotide phosphate induce pH changes in acidic Ca^{2+} stores in sea urchin eggs. *J. Biol. Chem.* 282:37730–37737. http://dx.doi.org/10.1074/jbc.M704630200

Morgan, A.J., and A. Galione. 2007b. NAADP induces pH changes in the lumen of acidic Ca^{2+} stores. *Biochem. J.* 402:301–310. http://dx.doi.org/10.1042/BJ20060759

Morgan, A.J., and A. Galione. 2008. Investigating cADPR and NAADP in intact and broken cell preparations. *Methods*. 46:194–203. http://dx.doi.org/10.1016/j.ymeth.2008.09.013

Morgan, A.J., and R. Jacob. 1994. Ionomycin enhances Ca^{2+} influx by stimulating store-regulated cation entry and not by a direct action at the plasma membrane. *Biochem. J.* 300:665–672.

Morgan, A.J., G.C. Churchill, R. Masgrau, M. Ruas, L.C. Davis, R.A. Billington, S. Patel, M. Yamasaki, J.M. Thomas, A.A. Genazzani, and A. Galione. 2006. Methods in cADPR and NAADP research. *In* Methods in Calcium Signalling. J.W. Putney, Jr., editor. CRC Press, Boca Raton. 265–334.

Morgan, A.J., F.M. Platt, E. Lloyd-Evans, and A. Galione. 2011. Molecular mechanisms of endolysosomal Ca^{2+} signalling in health and disease. *Biochem. J.* 439:349–374. http://dx.doi.org/10.1042/BJ20110949

Morgan, A.J., J. Parrington, and A. Galione. 2012. The luminal Ca^{2+} chelator, TPEN, inhibits NAADP-induced Ca^{2+} release. *Cell Calcium*. 52:481–487. http://dx.doi.org/10.1016/j.ceca.2012.09.001

Naraghi, M., and E. Neher. 1997. Linearized buffered Ca^{2+} diffusion in microdomains and its implications for calculation of $[Ca^{2+}]$ at the mouth of a calcium channel. *J. Neurosci.* 17:6961–6973.

Naylor, E., A. Arredouani, S.R. Vasudevan, A.M. Lewis, R. Parkesh, A. Mizote, D. Rosen, J.M. Thomas, M. Izumi, A. Ganesan, et al. 2009. Identification of a chemical probe for NAADP by virtual screening. *Nat. Chem. Biol.* 5:220–226. http://dx.doi.org/10.1038/nchembio.150

Nikolaev, V.O., M. Bünemann, L. Hein, A. Hannawacker, and M.J. Lohse. 2004. Novel single chain cAMP sensors for receptor-induced signal propagation. *J. Biol. Chem.* 279:37215–37218. http://dx.doi.org/10.1074/jbc.C400302200

Parys, J.B., S.M. McPherson, L. Mathews, K.P. Campbell, and F.J. Longo. 1994. Presence of inositol 1,4,5-trisphosphate receptor, calreticulin, and calsequestrin in eggs of sea urchins and *Xenopus laevis*. *Dev. Biol.* 161:466–476. http://dx.doi.org/10.1006/dbio.1994.1045

Patel, S., and E. Brailoiu. 2012. Triggering of Ca^{2+} signals by NAADP-gated two-pore channels: a role for membrane contact sites? *Biochem. Soc. Trans.* 40:153–157. http://dx.doi.org/10.1042/BST20110693

Patel, S., G.C. Churchill, and A. Galione. 2001. Coordination of Ca^{2+} signalling by NAADP. *Trends Biochem. Sci.* 26:482–489. http://dx.doi.org/10.1016/S0968-0004(01)01896-5

Pinton, P., A. Rimessi, A. Romagnoli, A. Prandini, and R. Rizzuto. 2007. Biosensors for the detection of calcium and pH. *Methods Cell Biol.* 80:297–325. http://dx.doi.org/10.1016/S0091-679X(06)80015-4

Pitt, S.J., T.M. Funnell, M. Sitsapesan, E. Venturi, K. Rietdorf, M. Ruas, A. Ganesan, R. Gosain, G.C. Churchill, M.X. Zhu, et al. 2010. TPC2 is a novel NAADP-sensitive Ca^{2+} release channel, operating as a dual sensor of luminal pH and Ca^{2+}. *J. Biol. Chem.* 285:35039–35046. http://dx.doi.org/10.1074/jbc.M110.156927

Poenie, M., and D. Epel. 1987. Ultrastructural localization of intracellular calcium stores by a new cytochemical method. *J. Histochem. Cytochem.* 35:939–956. http://dx.doi.org/10.1177/35.9.3611737

Ramos, I.B., K. Miranda, D.A. Pace, K.C. Verbist, F.Y. Lin, Y. Zhang, E. Oldfield, E.A. Machado, W. De Souza, and R. Docampo. 2010. Calcium- and polyphosphate-containing acidic granules of sea urchin eggs are similar to acidocalcisomes, but are not the targets for NAADP. *Biochem. J.* 429:485–495. http://dx.doi.org/10.1042/BJ20091956

Rizzuto, R., and T. Pozzan. 2006. Microdomains of intracellular Ca^{2+}: molecular determinants and functional consequences. *Physiol. Rev.* 86:369–408. http://dx.doi.org/10.1152/physrev.00004.2005

Ruas, M., K. Rietdorf, A. Arredouani, L.C. Davis, E. Lloyd-Evans, H. Koegel, T.M. Funnell, A.J. Morgan, J.A. Ward, K. Watanabe, et al. 2010. Purified TPC isoforms form NAADP receptors with distinct roles for Ca^{2+} signaling and endolysosomal trafficking. *Curr. Biol.* 20:703–709. http://dx.doi.org/10.1016/j.cub.2010.02.049

Rybalchenko, V., M. Ahuja, J. Coblentz, D. Churamani, S. Patel, K. Kiselyov, and S. Muallem. 2012. Membrane potential regulates nicotinic acid

adenine dinucleotide phosphate (NAADP) dependence of the pH- and Ca^{2+}-sensitive organellar two-pore channel TPC1. *J. Biol. Chem.* 287: 20407–20416. http://dx.doi.org/10.1074/jbc.M112.359612

Samsó, M., and T. Wagenknecht. 1998. Contributions of electron microscopy and single-particle techniques to the determination of the ryanodine receptor three-dimensional structure. *J. Struct. Biol.* 121:172–180. http://dx.doi.org/10.1006/jsbi.1997.3955

Sanjurjo, C.I., S.C. Tovey, D.L. Prole, and C.W. Taylor. 2012. Lysosomes shape IP_3-evoked Ca^{2+} signals by selectively sequestering Ca^{2+} released from the endoplasmic reticulum. *J. Cell Sci.* http://dx.doi.org/ 10.1242/jcs.116103

Santella, L., D. Lim, and F. Moccia. 2004. Calcium and fertilization: the beginning of life. *Trends Biochem. Sci.* 29:400–408. http://dx.doi.org/10.1016/j.tibs.2004.06.009

Santodomingo, J., L. Vay, M. Camacho, E. Hernández-Sanmiguel, R.I. Fonteriz, C.D. Lobatón, M. Montero, A. Moreno, and J. Alvarez. 2008. Calcium dynamics in bovine adrenal medulla chromaffin cell secretory granules. *Eur. J. Neurosci.* 28:1265–1274. http://dx.doi.org/10.1111/j.1460-9568.2008.06440.x

Sardet, C. 1984. The ultrastructure of the sea urchin egg cortex isolated before and after fertilization. *Dev. Biol.* 105:196–210. http://dx.doi.org/10.1016/0012-1606(84)90275-6

Shawl, A.I., K.H. Park, and U.H. Kim. 2009. Insulin receptor signaling for the proliferation of pancreatic β-cells: involvement of Ca^{2+} second messengers, IP3, NAADP and cADPR. *Islets*. 1:216–223. http://dx.doi.org/10.4161/isl.1.3.9646

Shen, S.S., and W.R. Buck. 1993. Sources of calcium in sea urchin eggs during the fertilization response. *Dev. Biol.* 157:157–169. http://dx.doi.org/10.1006/dbio.1993.1120

Shuai, J., and I. Parker. 2005. Optical single-channel recording by imaging Ca^{2+} flux through individual ion channels: theoretical considerations and limits to resolution. *Cell Calcium*. 37:283–299. http://dx.doi.org/10.1016/j.ceca.2004.10.008

Smith, I.F., and I. Parker. 2009. Imaging the quantal substructure of single IP_3R channel activity during Ca^{2+} puffs in intact mammalian cells. *Proc. Natl. Acad. Sci. USA*. 106:6404–6409. http://dx.doi.org/10.1073/pnas.0810799106

Steen, M., T. Kirchberger, and A.H. Guse. 2007. NAADP mobilizes calcium from the endoplasmic reticular Ca^{2+} store in T-lymphocytes. *J. Biol. Chem.* 282:18864–18871. http://dx.doi.org/10.1074/jbc.M610925200

Stern, M.D. 1992. Buffering of calcium in the vicinity of a channel pore. *Cell Calcium*. 13:183–192. http://dx.doi.org/10.1016/0143-4160(92)90046-U

Taylor, C.W., P.C. da Fonseca, and E.P. Morris. 2004. IP_3 receptors: the search for structure. *Trends Biochem. Sci.* 29:210–219. http://dx.doi.org/10.1016/j.tibs.2004.02.010

Terasaki, M., and L.A. Jaffe. 1991. Organization of the sea urchin egg endoplasmic reticulum and its reorganization at fertilization. *J. Cell Biol.* 114:929–940. http://dx.doi.org/10.1083/jcb.114.5.929

Thaler, C.D., R.C. Kuo, C. Patton, C.M. Preston, H. Yagisawa, and D. Epel. 2004. Phosphoinositide metabolism at fertilization of sea urchin eggs measured with a GFP-probe. *Dev. Growth Differ.* 46:413–423. http://dx.doi.org/10.1111/j.1440-169x.2004.00758.x

Thomas, J.M., R.J. Summerhill, B.R. Fruen, G.C. Churchill, and A. Galione. 2002. Calmodulin dissociation mediates desensitization of the cADPR-induced Ca^{2+} release mechanism. *Curr. Biol.* 12:2018–2022. http://dx.doi.org/10.1016/S0960-9822(02)01335-0

Treviño, C.L., J.L. De la Vega-Beltrán, T. Nishigaki, R. Felix, and A. Darszon. 2006. Maitotoxin potently promotes Ca^{2+} influx in mouse spermatogenic cells and sperm, and induces the acrosome reaction. *J. Cell. Physiol.* 206:449–456. http://dx.doi.org/10.1002/jcp.20487

Vasudevan, S.R., A.M. Lewis, J.W. Chan, C.L. Machin, D. Sinha, A. Galione, and G.C. Churchill. 2010. The calcium-mobilizing messenger NAADP participates in sperm activation by mediating the acrosome reaction. *J. Biol. Chem.* 285:18262–18269. http://dx.doi.org/10.1074/jbc.M109.087858

Whitaker, M. 2006. Calcium at fertilization and in early development. *Physiol. Rev.* 86:25–88. http://dx.doi.org/10.1152/physrev.00023.2005

Wolf, M., A. Eberhart, H. Glossmann, J. Striessnig, and N. Grigorieff. 2003. Visualization of the domain structure of an L-type Ca^{2+} channel using electron cryo-microscopy. *J. Mol. Biol.* 332:171–182. http://dx.doi.org/10.1016/S0022-2836(03)00899-4

Yamasaki, M., R. Masgrau, A.J. Morgan, G.C. Churchill, S. Patel, S.J. Ashcroft, and A. Galione. 2004. Organelle selection determines agonist-specific Ca^{2+} signals in pancreatic acinar and beta cells. *J. Biol. Chem.* 279:7234–7240. http://dx.doi.org/10.1074/jbc.M311088200

Yoshida, M., M. Ishikawa, H. Izumi, R. De Santis, and M. Morisawa. 2003. Store-operated calcium channel regulates the chemotactic behavior of ascidian sperm. *Proc. Natl. Acad. Sci. USA*. 100:149–154. http://dx.doi.org/10.1073/pnas.0135565100

Zhang, F., and P.L. Li. 2007. Reconstitution and characterization of a nicotinic acid adenine dinucleotide phosphate (NAADP)-sensitive Ca^{2+} release channel from liver lysosomes of rats. *J. Biol. Chem.* 282:25259–25269. http://dx.doi.org/10.1074/jbc.M701614200

Zong, X., M. Schieder, H. Cuny, S. Fenske, C. Gruner, K. Rötzer, O. Griesbeck, H. Harz, M. Biel, and C. Wahl-Schott. 2009. The two-pore channel TPCN2 mediates NAADP-dependent Ca^{2+}-release from lysosomal stores. *Pflugers Arch.* 458:891–899. http://dx.doi.org/10.1007/s00424-009-0690-y